

# Accepted Manuscript

Ionic Polymer Actuators Using Poly(ionic liquid) Electrolytes

Hisashi Kokubo, Ryo Sano, Keita Murai, Shunta Ishii, Masayoshi Watanabe

PII: S0014-3057(17)32052-9

DOI: <https://doi.org/10.1016/j.eurpolymj.2018.07.026>

Reference: EPJ 8488

To appear in: *European Polymer Journal*

Received Date: 17 November 2017

Revised Date: 8 July 2018

Accepted Date: 18 July 2018



Please cite this article as: Kokubo, H., Sano, R., Murai, K., Ishii, S., Watanabe, M., Ionic Polymer Actuators Using Poly(ionic liquid) Electrolytes, *European Polymer Journal* (2018), doi: <https://doi.org/10.1016/j.eurpolymj.2018.07.026>

This is a PDF file of an unedited manuscript that has been accepted for publication. As a service to our customers we are providing this early version of the manuscript. The manuscript will undergo copyediting, typesetting, and review of the resulting proof before it is published in its final form. Please note that during the production process errors may be discovered which could affect the content, and all legal disclaimers that apply to the journal pertain.

Special issue for “Poly(ionic liquid)s: innovative electrolytes for cutting-edge applications”

## **Ionic Polymer Actuators Using Poly(ionic liquid) Electrolytes**

Hisashi Kokubo, Ryo Sano, Keita Murai, Shunta Ishii, Masayoshi Watanabe \*

*Department of Chemistry and Biotechnology, Yokohama National University, 79-5 Tokiwadai,*

*Hodogaya-ku, Yokohama 240-8501, Japan*

\* Corresponding author

Tel & Fax: +81-45-339-3955

E-mail: [mwatanab@ynu.ac.jp](mailto:mwatanab@ynu.ac.jp)

## ABSTRACT

In this work, poly(ionic liquid) (polyIL) polymer electrolytes were prepared by the free radical copolymerization of IL monomers with a plasticizing monomer having poly(ethylene glycol) (PEG) side chain. The IL monomers, i.e., the polycation and polyanion precursors, were 1-[(3-methacryloyloxy)propyl]-3-methylimidazolium bis(trifluoromethanesulfonyl)amide ([C<sub>3</sub>mim-MA][TFSA]) and 1-methyl-3-propylimidazolium *N*-[3-(methacryloyloxy)propylsulfonyl]-*N*-(trifluoromethanesulfonyl)amide ([C<sub>3</sub>mim][TFSA-MA]), respectively. The ionic conductivities of the polyIL polymer electrolytes increased with a decrease in the weight fraction of the ionic monomer owing to the plasticizing effect of the PEG side chain, whereas the mechanical strength simultaneously decreased due to a lowering in the glass transition temperature of the electrolytes. The ionic conductivities of the electrolytes were 10<sup>-6</sup>–10<sup>-7</sup> S cm<sup>-1</sup> at room temperature. Ionic polymer actuators were fabricated using the polyILs as an electrolyte layer by sandwiching the electrolyte membrane with two carbon electrodes. The displacement behavior depended entirely on the fixed charge on the polymer chain.

Keywords:

Ionic liquid, Poly(ionic liquid), Polymer electrolyte, Single ion conductor, Ionic polymer actuator

## 1. Introduction

Electroactive polymers (EAPs) have attracted significant attention as indispensable materials for polymer actuators. In particular, polymer actuators utilizing ionic EAPs have certain advantages over electronic EAPs, such as low operation voltage ( $\approx 2$  V) and facile processability [1–6]. We have previously investigated ionic EAP actuators using polymer electrolytes consisting of an ionic liquid (IL) and a polymer [8–12]. The ILs are generally thermally and (electro)chemically stable, negligibly volatile, non-flammable, and highly ion-conductive [13–18], which are advantageous for fabricating ionic EAP actuators. Furthermore, the polymer electrolytes can afford mechanical integrity while maintaining the advantages of ILs [8,11,12,19]. The ionic polymer actuator can be driven even under vacuum owing to the negligible vapor pressure of the IL. Additionally, the mechanical strength of the polymer electrolytes is important for their durability [12].

The ionic polymer actuator is a kind of an electric double layer (EDL) capacitor. It undergoes deformation as a result of the ion migration from/to the electrodes accompanied with the charging of the EDL (Fig. 1). During the investigation of ion gel actuator, several factors affecting the actuator performance have come to light; the ionic conductivity of the ion gel influences the response speed, and the sizes and transference numbers of the cation and anion affect the magnitude of displacement and the bending direction. Thus, a model equation regarding the displacement of the actuator has been proposed [9]:

$$d = \frac{L^2}{3h} \frac{Q}{V_0} \frac{t_+v_+ - t_-v_-}{q} \quad (1)$$

where  $L$  and  $h$  are the length and thickness of the actuator, respectively;  $Q$  is the ionic charge accumulated at the EDL;  $V_0$  is the initial volume of the electrode;  $t_+$  and  $t_-$  refer to the cationic and anionic transference numbers, respectively;  $v_+$  and  $v_-$  indicate the volume of the cation and anion, respectively; and  $q$  is the elementary charge. The third term  $((t_+v_+ - t_-v_-)/q)$  indicates the difference in the electrode volume induced by charging of the EDL and determines the bending direction. Since  $t_+$  in the typical ion gels lies between 0.5 and 0.7 [12,19], the accumulated charge and the resulting volume changes are compensated between the cation and the anion. Therefore, it is of great interest to fabricate ionic polymer actuators by using polymer electrolytes that allow single-ion conduction. The transference number of a polyIL (polycation or polyanion) becomes unity depending on the fixed charge. Thus, Eq. (1) can be expressed by Eqs. (2) and (3) for the polycation and polyanion, respectively.

$$d = -\frac{L^2 Q v_-}{3h V_0 q} \quad (2)$$

$$d = \frac{L^2 Q v_+}{3h V_0 q} \quad (3)$$

Namely, the displacement depends entirely on the amount of accumulated charge and the volume of the counter ions. Typical polyILs have glass transition temperatures ( $T_g$ s) above room temperature, which results in relatively poor ionic conductivity for any electrochemical applications. However, it is possible to prepare polyILs having  $T_g$ s below room temperature via adequate molecular design [20–25].

In this work, we propose new polymer actuators using polyILs as an electrolyte layer. Compared to the conventional polymer actuators, these all-solid actuators are resistant to volatilization and leakage of the liquids even at an elevated temperature and under vacuum. For the preparation of the polycation and polyanion, 1-[(3-methacryloyloxy)propyl]-3-methylimidazolium bis(trifluoromethanesulfonyl)amide ([C<sub>3</sub>mimMA][TFSA]) and 1-methyl-3-propylimidazolium *N*-[3-(methacryloyloxy)propylsulfonyl]-*N*-(trifluoromethanesulfonyl)amide ([C<sub>3</sub>mim][TFSA-MA]), were synthesized, respectively. A reason for the selection of these monomers is relatively low  $T_g$  of the corresponding polymers [20, 24]. The polyILs were chemically cross-linked by ethylene glycol dimethacrylate (EGDMA) and copolymerized with poly(ethylene glycol) methyl ether methacrylate (PEGMEM) in order to further lower the  $T_g$  of the resulting polymer electrolytes. Polymer actuators utilizing the obtained polycation and polyanion membranes as an electrolyte layer were fabricated, and the fundamental performance such as magnitude of displacement and response speed was explored. The chemical structures of the compounds used in this study are given in **Fig. 2**.

## 2. Experimental part

### 2.1. Measurements

The differential scanning calorimetry (DSC) measurements were carried out on a Seiko Instruments DSC 6220 under N<sub>2</sub> atmosphere. The samples in sealed Al pans were first heated to 100 °C to remove thermal history, cooled to -150 °C, and then heated from -150 to 100 °C at a rate

of 10 °C min<sup>-1</sup>. DSC thermograms were recorded during the second heating scan. The tensile strength tests were conducted using a Shimadzu EX-X instrument at a cross-head speed of 6 mm min<sup>-1</sup>. The samples were cut into a rectangular piece of 30 mm length, 10 mm width, and 1 mm thickness, and the length of the clamped gap was 2 mm. The ionic conductivity was determined from complex impedance measurements using a Hewlett-Packard 4192LF impedance analyzer over a frequency range of 5 Hz – 13 MHz at an amplitude of 10 mV. The samples (thickness = 1 mm, diameter = 13 mm) were placed between two stainless steel disk electrodes.

## 2.2. Materials

Dehydrated dichloromethane (Wako), dehydrated tetrahydrofuran (THF) (Wako), *N*-methylpyrrolidone (NMP) (Wako), ethylene glycol dimethacrylate (EGDMA) (TCI), and poly(ethylene glycol) methyl ether methacrylate (PEGMEM) (average  $M_n = 500$ , Sigma-Aldrich) were used without further purification. 2,2'-Azobis(isobutyronitrile) (AIBN) (Wako) were purified by recrystallization from methanol prior to use.

## 2.3. Synthesis of the ionic monomers

The IL monomers were synthesized in accordance with **Scheme 1**. [C<sub>3</sub>mim-MA][TFSA] [26] and a precursor of [C<sub>3</sub>mim][TFSA-MA] (= [N<sub>0222</sub>][TFSA-MA]) [24] were synthesized accordingly to the previously reported literatures, and the detailed procedure was described in Supporting Information. 1-Methyl-3-propylimidazolium bromide ([C<sub>3</sub>mim]Br) was prepared from 1-methylimidazole and 1-bromopropane [27]. [C<sub>3</sub>mim][TFSA-MA] was synthesized as follows: [N<sub>0222</sub>][TFSA-MA] (16.7 g,

37.9 mmol) dissolved in dehydrated THF (30 mL) was added in a suspension solution consisting of dehydrated THF solution (30 mL) and [C<sub>3</sub>mim]Br (10.1 g, 49.3 mmol) under an argon atmosphere at 0 °C. After stirring for 12 h at 0 °C, the generated triethylammonium bromide was removed by filtration. THF was removed by evaporation, and the remaining solid was dissolved in 50 mL of dichloromethane. The solution was washed with water of 0 °C three times. The dichloromethane solution was dried by using magnesium sulfate, and the solvent was evaporated. Vacuum drying was conducted for 12 h at room temperature to afford [C<sub>3</sub>mim][TFSA-MA] as yellow viscous liquid (16.7 g, 45.1 mmol, Y = 43%). <sup>1</sup>H NMR (500 MHz, DMSO-*d*<sub>6</sub>) δ: 9.08 (s, 1H, N-CH-N), 7.76 and 7.70 (s, 2H, N-CH=CH-N), 6.04 and 5.68 (s, 2H, H<sub>2</sub>C=C(CH<sub>3</sub>)), 4.19 and 4.11 (m, 2H, O-CH<sub>2</sub>CH<sub>2</sub>CH<sub>2</sub>-S) and (m, 2H, N-CH<sub>2</sub>CH<sub>2</sub>CH<sub>3</sub>), 3.85 (s, 3H, N-CH<sub>3</sub>), 3.08 (t, 2H, O-CH<sub>2</sub>CH<sub>2</sub>CH<sub>2</sub>-S), 2.04 (m, 2H, O-CH<sub>2</sub>CH<sub>2</sub>CH<sub>2</sub>-S), 1.88 (t, 3H, H<sub>2</sub>C=C(CH<sub>3</sub>)), 1.79 (m, 2H, N-CH<sub>2</sub>CH<sub>2</sub>CH<sub>3</sub>), 0.86 (t, 3H, N-CH<sub>2</sub>CH<sub>2</sub>CH<sub>3</sub>). <sup>13</sup>C NMR (125 MHz, DMSO-*d*<sub>6</sub>) δ: 166.4 (C=O), 136.5 (N-CH-N), 135.8 (CH<sub>2</sub>=C(CH<sub>3</sub>)), 125.7 (CH<sub>2</sub>=C(CH<sub>3</sub>)), 123.6 and 122.2 (N-CH=CH-N), 121.4 and 118.8 (CF<sub>3</sub>), 62.7 (O-CH<sub>2</sub>CH<sub>2</sub>CH<sub>2</sub>-S), 51.2 (O-CH<sub>2</sub>CH<sub>2</sub>CH<sub>2</sub>-S), 50.3 (N-CH<sub>2</sub>CH<sub>2</sub>CH<sub>3</sub>), 35.7 (N-CH<sub>3</sub>), 23.5 (O-CH<sub>2</sub>CH<sub>2</sub>CH<sub>2</sub>-S), 22.7 (N-CH<sub>2</sub>CH<sub>2</sub>CH<sub>3</sub>), 17.9 (CH<sub>2</sub>=C(CH<sub>3</sub>)), 10.3 (N-CH<sub>2</sub>CH<sub>2</sub>CH<sub>3</sub>).

<sup>1</sup>H and <sup>13</sup>C NMR spectra of the synthesized intermediates and final products (ionic monomers) are shown in **Figure S1–S12**.

#### 2.4. Preparation of cross-linked polyIL membranes

The polymer networks include a given ratio of PEGMEM (internal plasticizing monomer) segment. The weight ratio of the ionic monomer ([C<sub>3</sub>mim-MA][TFSA] for the polycation and [C<sub>3</sub>mim][TFSA-MA] for the polyanion) has been represented as  $x$  (= 0.5–1.0) hereafter. A mixture consisting of [C<sub>3</sub>mim-MA][TFSA] for polycation or [C<sub>3</sub>mim][TFSA-MA] for polyanion, PEGMEM as an internal plasticizer, AIBN as an initiator, and EGDMA as a cross-linker after argon bubbling for 30 min was placed on a polyethylene terephthalate (PET) sheet separated by Teflon spacer. The compositions of each reagent are summarized in **Table S1** and **S2** in Supporting Information. The feed content of EGDMA was decided to be 2 mol% of the total monomers. After placing the sample at 80 °C for 24 h for polymerization and then at 120 °C for 4 h for the completion, the polymer membranes were obtained.

### 2.5. Fabrication of polymer actuator samples and actuator tests

In order to prepare carbon electrodes consisting of the polyILs, 13 wt% of activated carbon, 22 wt% of acetylene black, and 65 wt% of the polyIL (homopolymer without the inner plasticizing segment) were mixed with NMP by using a planetary centrifugal mixer AR-310 (THINKY) for 20 min and then degassed for 10 min. The obtained slurries were coated on PET sheets with a thickness of 50  $\mu\text{m}$  by using a K Control Coater print applicator (RK Print Coat Instruments). After vacuum drying at 60 °C for 12 h and then at 80 °C for 12 h, carbon electrode sheets having a thickness of 20–25  $\mu\text{m}$  were obtained. The electrode sheet showed an electric resistivity of 3–4  $\Omega\text{ cm}$ , as measured by the four-probe method using a Loresta GP MSP-T610 resistivity meter (Mitsubishi

Chemical Analytech). The electrode sheets were used for the polyIL actuator. The cross-linked polyIL films ( $x = 0.7$ ) were sandwiched by the carbon electrodes containing the corresponding polyIL, and the composites were moderately pressed at 170 °C for 10 min. The prepared composite films were cut into a  $2 \times 7$  mm rectangular shape for their evaluation as a polymer actuator.

The cut actuator sample was clamped by two current collectors made of stainless steel and connected to a potentiostat HA-301 and a function generator HB-104 (HOKUTO DENKO). The displacement was measured by a laser displacement meter LC-2440 (KEYENCE) placed at a distance of 4 mm from the clamped end. The measurements were performed under ambient atmosphere three times for each polyIL actuator.

### 3. Results and discussion

#### 3.1. Characterization of synthesized IL monomers and fabrication of polyIL networks

The IL monomers ( $[\text{C}_3\text{mim-MA}][\text{TFSA}]$  and  $[\text{C}_3\text{mim}][\text{TFSA-MA}]$ ) were prepared via a three step synthetic procedure, as shown in **Scheme 1**. The products of all the steps were characterized by  $^1\text{H}$  and  $^{13}\text{C}$  NMR (**Figs. S1–S12** in Supporting Information). The polymerization reaction was conducted via free radical polymerization at 80 °C. The temperature was relatively high for radical polymerization using AIBN. This was due to the reduction of viscosity of the viscous ionic monomers. The reaction samples were then placed at 120 °C for 4 h in order to completely decompose the remaining AIBN in the polymer electrolytes. To confirm the consumption of the

monomers and the completion of the polymerization reaction, we carried out Fourier transform infrared (FT-IR) analysis of the resultant polymer network and  $^1\text{H}$  NMR analysis of a  $\text{DMSO-}d_6$  solution of the polyanion network extract, which was prepared by soaking of the polyanion network (ca. 50 mg) in  $\text{DMSO-}d_6$  (2 mL) for 12 h with gentle shaking. **Fig. S13** shows FT-IR spectrum of the resultant polyanion network with  $x$  value of 0.9 measured by attenuated total reflection (ATR) method. A specific absorption band assigned to C=C stretching at  $1640\text{ cm}^{-1}$  was not observed. In addition, **Fig. S14** displays  $^1\text{H}$  NMR spectrum of a  $\text{DMSO-}d_6$  solution of the polyanion network extract with  $x = 0.9$ . NMR signals of certain polymers resulting from the ionic monomer and PEGMEM were observed, indicating that linear polymers, which did not participate in the polymer network, existed in the cross-linked polymer. However, no signals assigned to  $\text{H}_2\text{C}=\text{C}-$  were observed between  $\delta$  5.5–6.2. These results (FT-IR spectrum and  $^1\text{H}$  NMR spectrum) indicate that no unreacting ionic monomers, PEGMEM, and EGDMA, exist in the polyanion network. The amount of linear polymer was estimated by weight of polyanion with  $x$  value of 0.9 before and after washing with acetonitrile for 12 h. Accordingly, 4 wt% linear polymer was extracted from polyanion network. However, we consider that the linear polymer does not greatly contribute the increase in ionic conductivity. The polymer networks consisting of only IL monomers showed high  $T_g$ s and low ionic conductivities (*vide infra*). In order to improve their conductivity, we performed the copolymerization between the ionic monomers and the internal plasticizing monomer with a given weight ratio. The polymer network with the IL monomer content  $x < 0.5$  could not be obtained as a

self-standing film.

### 3.2. DSC measurements and tensile tests

The DSC curves of the fabricated polycation and polyanion networks consisting of the IL monomer and inner plasticizing monomer are shown in **Fig. 3(a)** and **(b)**, respectively, and the correlation between the weight fraction of the ionic segment ( $x$ ) and the  $T_g$ s of the network have been summarized in **Fig. 3(c)**. In both the polycation and polyanion systems, an increase in  $T_g$  was observed with an increase in the value of  $x$  (weight ratio of the IL monomer). These results indicated that the PEG side chain in PEGMEM effectively functioned as an internal plasticizer in the polymer networks. The  $T_g$ s of the polycation networks were higher than those of the polyanion networks in the entire range of  $x$  (from 0.5 to 1.0). As the alkyl spacer between the main chain and the ionic part were unified as propylene ( $-(CH_2)_3-$ ), the differences in the  $T_g$ s may result from the structure of the ionic part. While the imidazolium ring with its planar structure has a lesser degree of conformational freedom, the TFSA anion is flexible and can undergo conformational change. As a result, the polyanion networks had lower  $T_g$ s compared to the polycation networks [20,22].

The stress-strain curves of the polycation and polyanion networks are shown in **Fig. 4**, and the elastic moduli (Young's moduli), fracture stress, fracture strains, and fracture energies are summarized in **Table 1**. In both polycation and polyanion networks, the elastic moduli were almost the same value because the cross-linking density was identical. In contrast, the fracture strain and the fracture energy increase with an increase in  $x$  possibly due to the increase in  $T_g$ , resulting in an

increase in the deformability. Similar behavior has been observed for copolymers of ionic and non-ionic monomers [28].

### 3.3. Ionic conductivity

The Arrhenius plots of the ionic conductivity for the polycation and polyanion networks are shown in **Fig. 5(a)** and **(b)**, and the ionic conductivity (at 30 °C) as a function of  $x$  is displayed in **Fig. 5(c)**. Here, note that the counterions of polyILs mostly contribute the ionic conductivity because ionic monomers do not exist in the polymer networks. The ionic conductivities of both polymer electrolytes at room temperature were of the order of  $10^{-6}$ – $10^{-7}$  S cm<sup>-1</sup>. Although the density of ionic group in the both polymer networks decreases, their ionic conductivity increased with a decrease in  $x$ . This result indicates that the plasticizing effect of the PEG side chain resulting from lowered  $T_g$  likely contributed to the enhancement of the carrier mobility [23,29]. Another possibility can be the carrier density enhancement effect by the introduction of the PEG chain. The carrier density could be increased by the addition of PEG because of its solvation power that facilitates ionic dissociation [30]. The temperature dependence of the ionic conductivity can be represented by the Vogel-Tamman-Fulcher (VTF) equation as follows:

$$\sigma(T) = \sigma_0 \exp \left[ \frac{-B}{T - T_0} \right] \quad (4)$$

where  $\sigma_0$  (S cm<sup>-1</sup>),  $B$  (K), and  $T_0$  (K) are the fitting parameters. The values of these parameters have been summarized in **Table 2**. The ionic conductivity of the polyanion networks was higher than that of the polycation networks irrespective of the  $x$  value (**Fig. 5(c)**), which is in accordance with the

lower  $T_g$ s of the polyanion networks as compared to those of the polycation networks (**Fig. 3(c)**). In the case of the ionic liquids consisting of an imidazolium cation and TFSA anion in a PEG matrix, we found that the transference number of the cation is higher than that of the anion by means of pulsed-field spin-echo NMR [12]. Therefore, the facile movement of the imidazolium cation may also contribute to the higher ionic conductivity of the polyanion.

#### 3.4. Performance of polymer actuator using polyIL networks

We used polyILs with  $x = 0.7$  as the electrolyte layer of the fabricated polymer actuators because they relatively have both high ionic conductivities and mechanical strength, compared to the polyILs having different  $x$  values. **Fig. 6** shows the current and displacement responses of the actuators on the application of  $\pm 2$  V rectangular wave voltage with frequency of 0.01 Hz. The typical charging current of the EDL was observed as soon as the polarity of the applied voltage was changed. The charging current of the polyanion network ( $41 \mu\text{A}$  at 1 s) was larger than that of polycation system ( $14 \mu\text{A}$  at 1 s) as a result of the difference in the ionic conductivities of the electrolyte membranes. The maximum displacements of the polycation and polyanion networks during 1–50 s were  $-70 \mu\text{m}$  and  $+92 \mu\text{m}$ , respectively. Here, the sign of the displacement implies the direction of bending, where these bending behaviors can be well-explained by using Eqs. (2) and (3). To confirm the duration of the displacement behavior, long-time voltage application tests were conducted. **Fig. 7(a)** shows the current and displacement behavior under the application of  $+2$  V for 2000 s. Because of low ionic conductivity of the electrolytes ( $10^{-6}$ – $10^{-7} \text{ Scm}^{-1}$ ), the charging of the EDL was slow. Therefore, the

displacement also gradually increased in both actuators. The relationship between the accumulated electric charge and displacement is shown in **Fig. 7(b)**. The dashed lines indicate the calculated values from Eqs. (2) and (3), using ionic sizes of 127 and 147 Å<sup>3</sup> for the [C<sub>3</sub>mim] cation and the [TFSA] anion, respectively [31]. While both actuators showed good agreement with the calculated displacements in the low charge region, the experimental displacements strayed off from the calculated line with an increase in the accumulated charge. In this type of an actuator, such phenomena were often observed [9,12], and were a result of localized bending at the root of the actuator sample occurring because of the low electric conductivity of the carbon electrodes and low ionic conductivity of the polymer electrolytes. Owing to the low ionic conductivity, the polymer actuators showed a slow response for more than 2000 s until the bending behavior reached the maximum displacement. Ionic polymer actuators with ionic liquids having high ionic conductivities ( $10^{-2}$ – $10^{-3}$  S cm<sup>-1</sup>) typically show a fast response, reaching saturated deformation within 30 s [8,10,12]. Therefore, an increase in the ionic conductivity of the polymer electrolyte is required in order to improve the response speed. However, in this paper, we successfully demonstrated the application of polyIL electrolytes with single-ion conduction to ionic polymer actuators, which do not contain any evaporating solvents.

#### 4. Conclusions

In this work, solid polymer electrolytes consisting of polyIL networks were prepared by free

radical copolymerization using an IL monomer and an internal plasticizing monomer. Both polymer electrolytes (polycation and polyanion networks) showed ionic conductivities of  $10^{-6}$ – $10^{-7}$  S cm<sup>-1</sup> at room temperature. A decrease in the value of  $x$  caused a decrease in the  $T_g$  and an increase in the ionic conductivity. At the same time, as the  $x$  value decreased, the mechanical strength of the polymer electrolytes also decreased. To maintain a sufficient mechanical strength and ionic conductivity, the polymer electrolytes with  $x = 0.7$  were applied to the polymer actuator as the electrolyte layer. The bending behavior of the polycation and the polyanion actuators depended entirely on the fixed charge on the polymer network and could be explained by using Eqs. (2) and (3). In order to improve the actuation speed, an increase in the ionic conductivity for the solid polymer electrolytes is required while maintaining adequate mechanical strength. In this article, we showed the fundamental performance of the polymer actuators utilizing the obtained polyILs, and could elucidate the bending behavior by using model equations (Eqs. (2) and (3)). In future, we need further refinement for long cycle life, large displacement and generating force, and high actuation speed.

### **Acknowledgments**

This work was partly supported by the Grants-in-Aid for Scientific Research (S 15H05758) and the grants for Specially Promoted Research on “Iontronics” from Ministry of Education, Culture, Sports, Science and Technology (MEXT) of Japan.

**Appendix A. Supplementary material**

Supplementary data associated with this article can be found, in the online version, at <http://dx.doi.org/10.1016/j.eurpolymj.xxxx.xx.xxx>.

ACCEPTED MANUSCRIPT

**References**

- [1] K. Kaneto, M. Kaneko, M. Min, A.G. MacDiamid, “Artificial muscle”: Electrochemical actuators using polyaniline films, *Synth. Met.* 71 (1995) 2211–2212.
- [2] R.H. Baughman, Conducting polymer artificial muscles, *Synth. Met.* 78 (1996) 339–353.
- [3] E. Smela, Conjugated polymer actuators for biomedical applications, *Adv. Mater.* 15 (2003) 481–494.
- [4] R.H. Baughman, C. Cui, A.A. Zakhidov, Z. Iqbal, J.N. Barisci, G.M. Spinks, G.G. Wallace, A. Mazzoldi, D.D. Rossi, A.G. Rinzler, O. Jaschinski, S. Roth, M. Kertesz, Carbon nanotube actuators, *Science* 284 (1999) 1340–1344.
- [5] K. Asaka, K. Oguro, Y. Nishimura, M. Mizuhata, H. Takenaka, Bending of polyelectrolyte membrane–platinum composites by electric stimuli I. Response characteristics to various waveforms, *Polym. J.* 27 (1995) 436–440.
- [6] M. Shahinpoor, Ionic polymer–conductor composites as biomimetic sensors, robotic actuators and artificial muscles—a review, *Electrochim. Acta* 48 (2003) 2343–2353.
- [7] R. Mejri, J.C. Dias, S.B. Hentati, G. Botelho, J.M.S.S. Esperança, C.M. Costa, S. Lanceros-Mendez, Imidazolium-based ionic liquid type dependence of the bending response of polymer actuators, *Eur. Polym. J.* 85 (2016) 445–451.
- [8] S. Imaizumi, H. Kokubo, M. Watanabe, Polymer actuators using ion-gel electrolytes prepared by self-assembly of ABA-triblock copolymers, *Macromolecules* 45 (2012) 401–409.
- [9] S. Imaizumi, Y. Kato, H. Kokubo, M. Watanabe, Driving mechanism of ionic polymer actuators having electric double layer capacitor structures, *J. Phys. Chem. B* 116 (2012) 5080–5089.
- [10] S. Imaizumi, Y. Ohtsuki, T. Yasuda, H. Kokubo, M. Watanabe, Printable polymer actuators from ionic liquid, soluble polyimide, and ubiquitous carbon materials, *ACS Appl. Mater. Interfaces* 5 (2013) 6307–6315.
- [11] H. Kokubo, T. Honda, S. Imaizumi, K. Dokko, M. Watanabe, Effects of carbon electrode

- materials on performance of ionic polymer actuators having electric double-layer capacitor structure, *Electrochemistry* 81 (2013) 849–852.
- [12] S. Ishii, H. Kokubo, K. Hashimoto, S. Imaizumi, M. Watanabe, Tetra-PEG network containing ionic liquid synthesized via Michael addition reaction and its application to polymer actuator, *Macromolecules* 50 (2017) 2906–2915.
- [13] T. Welton, Room-temperature ionic liquids. Solvents for synthesis and catalysis, *Chem. Rev.* 99 (1999) 2071–2084.
- [14] J.D. Holbrey, K.R. Seddon, Ionic liquids, *Clean Technol. Environ. Policy* 1 (1999) 223–236.
- [15] P. Wasserscheid, W. Keim, Ionic liquids—New “solutions” for transition metal catalysis, *Angew. Chem., Int. Ed.* 39 (2000) 3772–3789.
- [16] J.S. Wilkes, A short history of ionic liquids—From molten salts to neoteric solvents, *Green Chem.* 4 (2002) 73–80.
- [17] K.R. Seddon, Ionic liquids: A taste of the future, *Nat. Mater.* 2 (2003) 363–365.
- [18] N.V. Plechkova, K.R. Seddon, Applications of ionic liquids in the chemical industry, *Chem. Soc. Rev.* 37 (2008) 123–150.
- [19] M.A.B.H. Susan, T. Kaneko, A. Noda, M. Watanabe, Ion gels prepared by in situ radical polymerization of vinyl monomers in an ionic liquid and their characterization as polymer electrolytes, *J. Am. Chem. Soc.* 127 (2005) 4976–4983.
- [20] A.S. Shaplov, E.I. Lozinskaya, D.O. Ponkratov, I.A. Malyshkina, F. Vidal, P.-H. Aubert, O.V. Okatova, G.M. Pavlov, L.I. Komarova, C. Wandrey, Y.S. Vygodskii, Bis(trifluoromethylsulfonyl)amide based “polymeric ionic liquids”: Synthesis, purification and peculiarities of structure–properties relationships, *Electrochim. Acta* 57 (2011) 74–90.
- [21] A.S. Shaplov, P.S. Vlasov, E.I. Lozinskaya, D.O. Ponkratov, I.A. Malyshkina, F. Vidal, O.V. Okatova, G.M. Pavlov, C. Wandrey, A. Bhide, M. Schönhoff, Y.S. Vygodskii, Polymeric ionic liquids: Comparison of polycations and polyanions, *Macromolecules* 44 (2011) 9792–9803.

- [22] A.S. Shaplov, D.O. Ponkratov, P.S. Vlasov, E.I. Lozinskaya, L.I. Komarova, I.A. Malyshkina, F. Vidal, G.T.M. Nguyen, M. Armand, C. Wandrey, Y.S. Vygodskii, Synthesis and properties of polymeric analogs of ionic liquids, *Polym. Sci. Ser. B* 55 (2013) 122–138.
- [23] H. Chen, J.-H. Choi, D.S. Cruz, K.I. Winey, Y.A. Elabd, Polymerized ionic liquids: The effect of random copolymer composition on ion conduction, *Macromolecules* 42 (2009) 4809–4816.
- [24] A.S. Shaplov, P.S. Vlasov, M. Armand, E.I. Lozinskaya, D.O. Ponkratov, I.A. Malyshkina, F. Vidal, O.V. Okatova, G.M. Pavlov, C. Wandrey, I.A. Godovikov, Y.S. Vygodskii, Design and synthesis of new anionic “polymeric ionic liquids” with high charge delocalization, *Polym. Chem.* 2 (2011) 2609–2618.
- [25] A. Eftekharia, T. Saito, Synthesis and properties of polymerized ionic liquids, *Eur. Polym. J.* 90 (2017) 245–272.
- [26] A.S. Shaplov, L. Goujon, F. Vidal, E.I. Lozinskaya, F. Meyer, I.A. Malyshkina, C. Chevrot, D. Teyssié, I.L. Odinet, Y.S. Vygodskii, Ionic IPNs as novel candidates for highly conductive solid polymer electrolytes, *J. Polym. Sci. Part A: Polym. Chem.* 47 (2009) 4245–4266.
- [27] E.A. Turner, C.C. Pye, R.D. Singer, Use of ab Initio Calculations toward the Rational Design of Room Temperature Ionic Liquids, *J. Phys. Chem. A* 107 (2003) 2277–2288.
- [28] P. Guo, H. Zhang, X. Liu, J. Sun, Counteranion-mediated intrinsic healing of poly(ionic liquid) copolymers, *ACS Appl. Mater. Interfaces* 10 (2018) 2105–2113.
- [29] H. Hu, W. Yuan, Z. Jia, G.L. Baker, Ionic liquid-based random copolymers: a new type of polymer electrolyte with low glass transition temperature, *RSC Adv.* 5 (2015) 3135–3140.
- [30] A.S. Lee, J.H. Lee, S.M. Hong, J.-C. Lee, S.S. Hwang, C.M. Koo, Ion conduction behaviour in chemically crosslinked hybrid ionogels: effect of free-dangling oligoethyleneoxides, *RSC Adv.* 5 (2015) 94241–94247.
- [31] W. Beichel, P. Eiden, I. Krossing, Establishing consistent van der Waals volumes of polyatomic ions from crystal structures, *ChemPhysChem* 14 (2013) 3221–3226.

## Captions for Figures

**Scheme 1** Synthetic route for IL monomers.

**Fig. 1.** Schematic images of (a) structure of polymer actuator in this study and (b) driving mechanism of the polymer actuator using ionic liquids or ionic salts as an electrolyte in the case of ( $t_+ > t_-$ ); (i) before applying voltage, (ii) after applying voltage, ion migration to both EDL associated with charging, (iii) deformation toward positive electrode due to the increase in the volume of negative electrode.

**Fig. 2.** Scheme for preparation of polyIL networks and the chemical structures of the monomers, internal plasticizing monomer, and cross-linking agent used in this study.

**Fig. 3.** DSC curves of the (a) polycation and (b) polyanion networks with different  $x$ . (c)  $T_g$ s for the polycation and polyanion networks as a function of  $x$ .

**Fig. 4.** Stress-strain curves of the (a) polycation and (b) polyanion networks with different weight percent of the IL monomer.

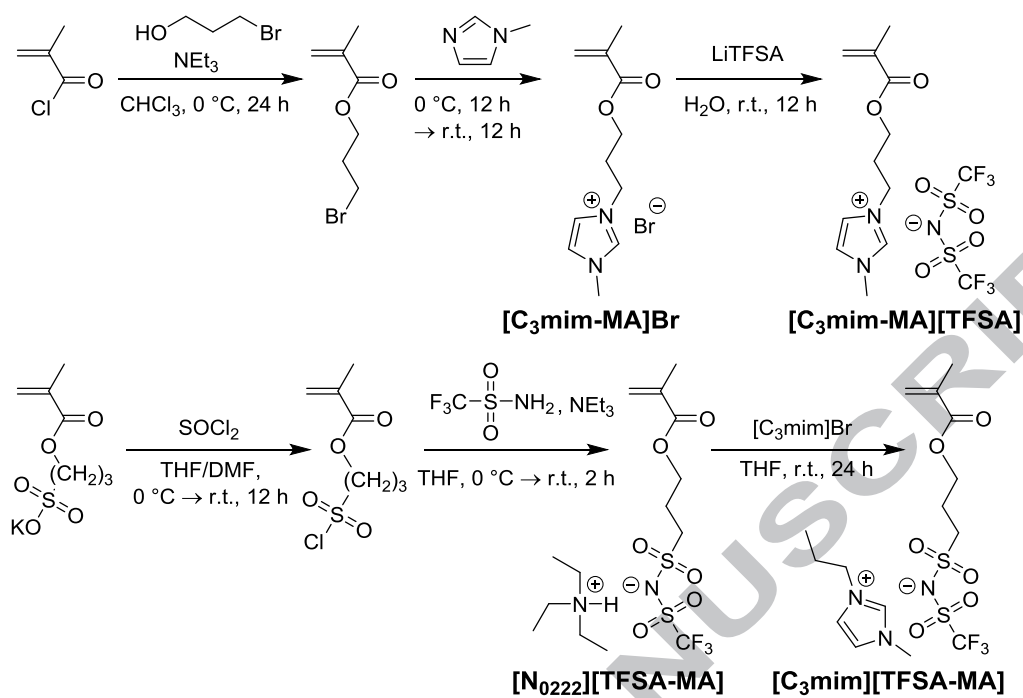
**Fig. 5.** Temperature dependence of the ionic conductivities of the (a) polycation and (b) polyanion networks with different  $x$ , and the (c) ionic conductivities of the polycation and polyanion networks at 25 °C as a function of  $x$ .

**Fig. 6.** Current and displacement responses of the polymer actuator to an applied  $\pm 2$  V rectangular wave with a frequency of 0.01 Hz using the polycation (red) and polycation (blue) networks as the electrolyte ( $x = 0.7$ ).

**Fig. 7.** (a) Current and displacement responses of the polymer actuator using the polycation (red) and polycation (blue) networks as the electrolyte with the application of an applied voltage of +2 V ( $x = 0.7$ ). (b) Displacement of the polycation and polyanion actuators against the amount of the

accumulated charge (solid line) and the calculated displacement (dashed line), as determined by Eqs. (2) and (3) for the polycation and polyanion actuators, respectively.

ACCEPTED MANUSCRIPT



Scheme 1 Synthetic route for IL monomers.

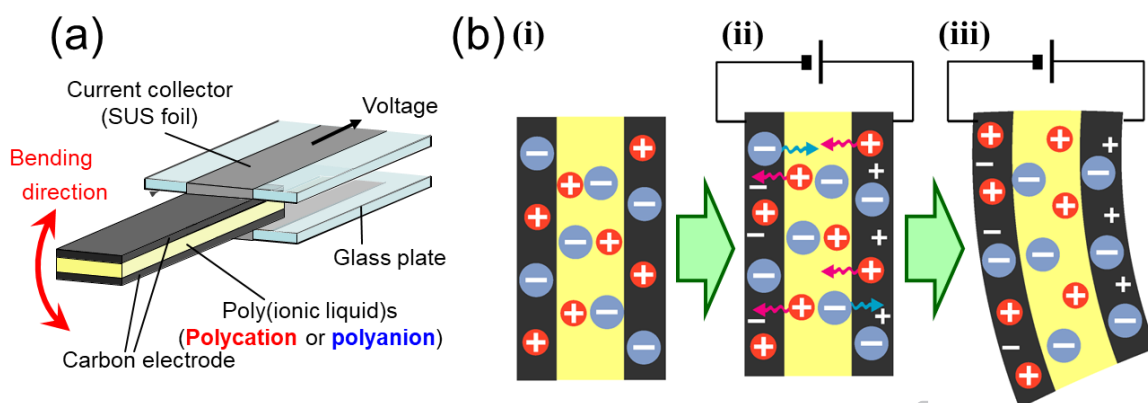


**Fig. 1.** Schematic images of (a) structure of polymer actuator in this study and (b) driving mechanism of the polymer actuator using ionic liquids or ionic salts as an electrolyte in the case of ( $t_+ > t_-$ ); (i) before applying voltage, (ii) after applying voltage, ion migration to both EDL associated with charging, (iii) deformation toward positive electrode due to the increase in the volume of negative electrode.

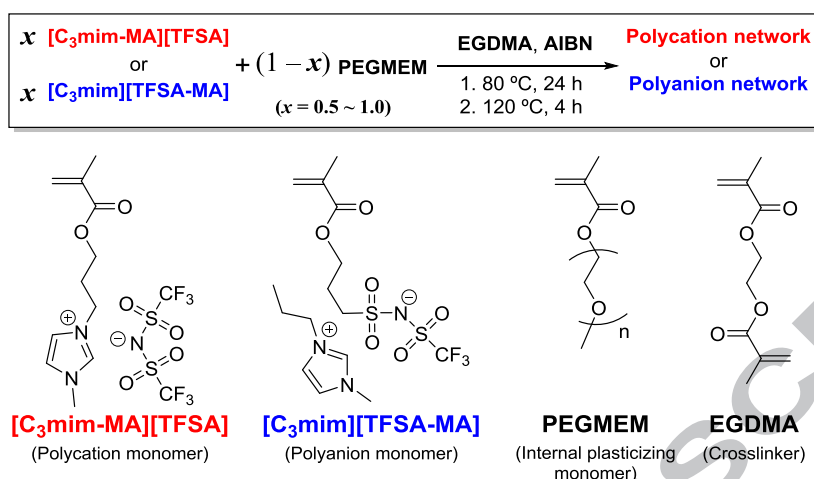


**Fig. 2.** Scheme for preparation of polyIL networks and the chemical structures of the monomers, internal plasticizing monomer, and cross-linking agent used in this study.

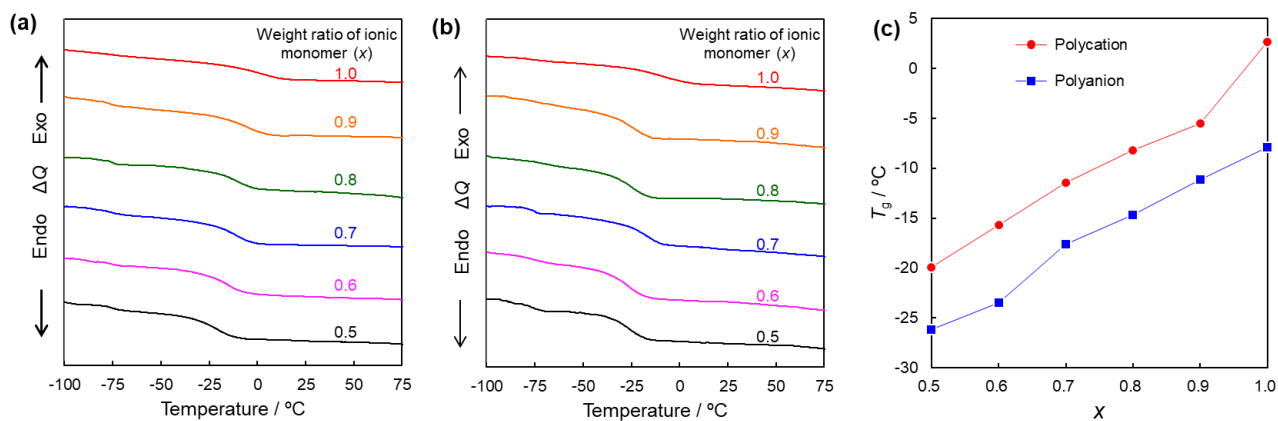


**Fig. 3.** DSC curves of the (a) polycation and (b) polyanion networks with different  $x$ . (c)  $T_g$ s for the polycation and polyanion networks as a function of  $x$ .

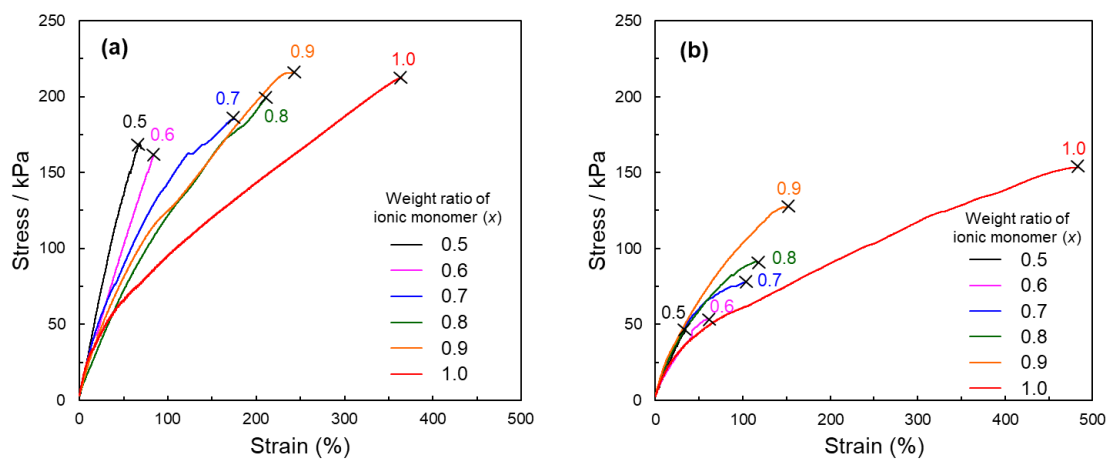


**Fig. 4.** Stress-strain curves of the (a) polycation and (b) polyanion networks with different weight percent of the IL monomer.

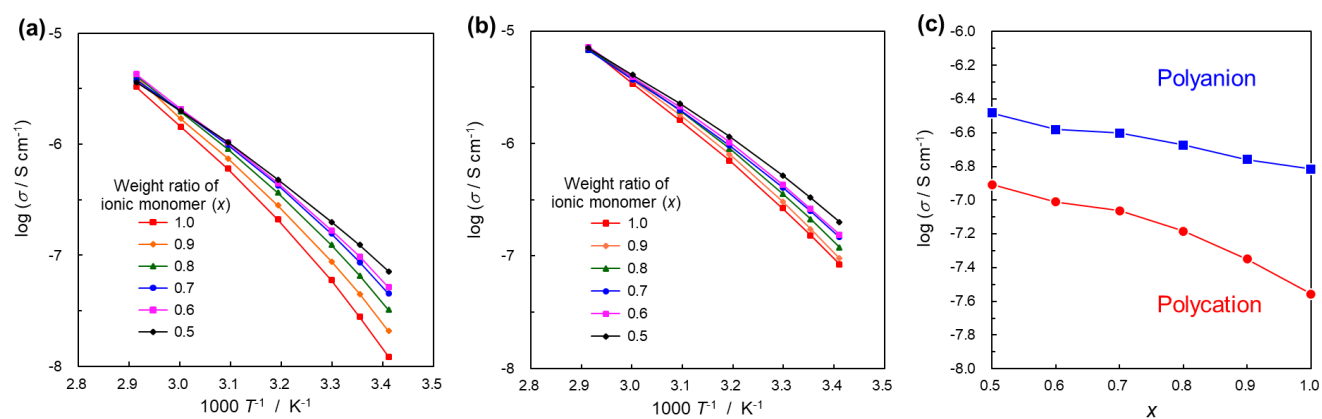


**Fig. 5.** Temperature dependence of the ionic conductivities of the (a) polycation and (b) polyanion networks with different  $x$ , and the (c) ionic conductivities of the polycation and polyanion networks at 25 °C as a function of  $x$ .

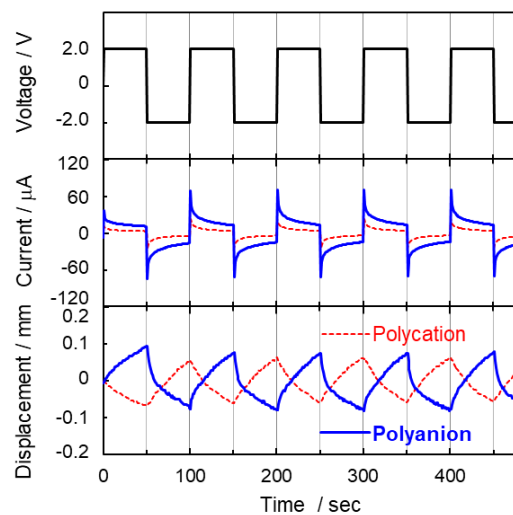


**Fig. 6.** Current and displacement responses of the polymer actuator to an applied  $\pm 2$  V rectangular wave with a frequency of 0.01 Hz using the polycation (red) and polyanion (blue) networks as the electrolyte ( $x = 0.7$ ).

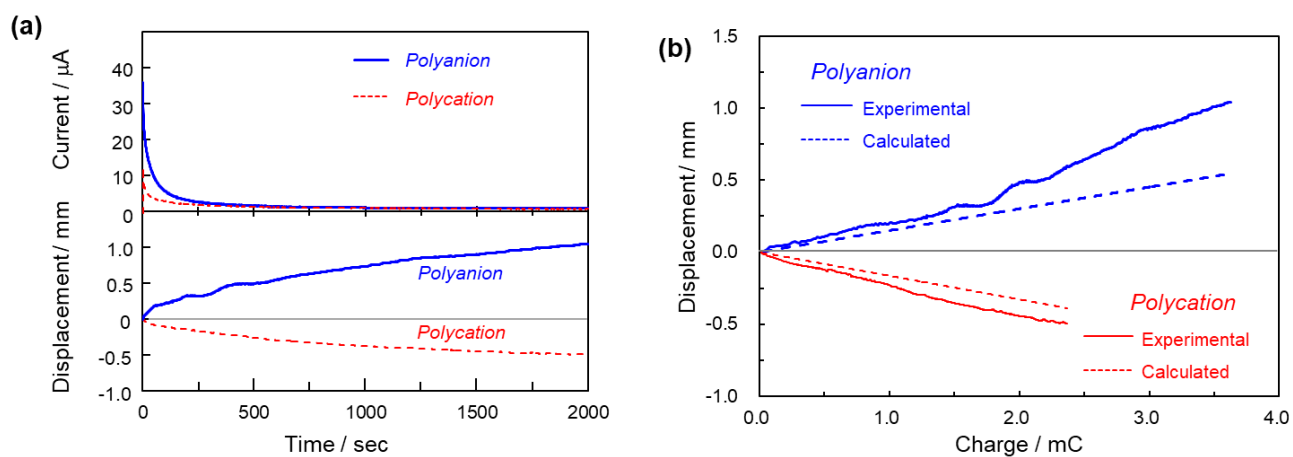


**Fig. 7.** (a) Current and displacement responses of the polymer actuator using the polycation (red) and polyanion (blue) networks as the electrolyte with the application of an applied voltage of +2 V ( $x = 0.7$ ). (b) Displacement of the polycation and polyanion actuators against the amount of the accumulated charge (solid line) and the calculated displacement (dashed line), as determined by Eqs. (2) and (3) for the polycation and polyanion actuators, respectively.

**Table 1** Mechanical properties and ionic conductivities of the polyIL networks at 25 °C.

Weight ratio of ionic monomer ( <i>x</i> )	Polycation					Polyanion				
	<i>E</i> / kPa <sup>a)</sup>	F. Stress / kPa <sup>b)</sup>	F. Strain (%) <sup>c)</sup>	FE / kJ m <sup>-3</sup> <sup>d)</sup>	$\sigma_{RT}$ / Scm <sup>-1</sup> <sup>e)</sup>	<i>E</i> / kPa <sup>a)</sup>	F. Stress / kPa <sup>b)</sup>	F. Strain (%) <sup>c)</sup>	FE / kJ m <sup>-3</sup> <sup>d)</sup>	$\sigma_{RT}$ / Scm <sup>-1</sup> <sup>e)</sup>
1.0	268	213	365	477	$2.8 \times 10^{-8}$	180	153	483	471	$1.5 \times 10^{-7}$
0.9	268	216	242	328	$4.5 \times 10^{-8}$	147	127	152	123	$1.7 \times 10^{-7}$
0.8	278	199	211	249	$6.5 \times 10^{-8}$	175	91	118	72	$2.1 \times 10^{-7}$
0.7	171	185	176	214	$8.7 \times 10^{-8}$	179	78	104	45	$2.5 \times 10^{-7}$
0.6	217	162	84	73	$9.7 \times 10^{-8}$	210	54	60	11	$2.6 \times 10^{-7}$
0.5	280	169	68	66	$1.2 \times 10^{-7}$	166	47	35	9	$3.3 \times 10^{-7}$

<sup>a)</sup> Elastic (Young's) modulus, <sup>b)</sup> fracture stress, <sup>c)</sup> fracture strain, <sup>d)</sup> fracture energy, <sup>e)</sup> ionic conductivity at 25 °C.

**Table 2** Fitting parameters of the VTF equation for determining the ionic conductivity of polyIL networks.

Weight ratio of ionic monomer ( $x$ )	Polycation				Polyanion			
	$\sigma_0$ (S cm <sup>-1</sup> )	$B$ (10 <sup>2</sup> K)	$T_0$ (K)	$R^2$	$\sigma_0$ (S cm <sup>-1</sup> )	$B$ (10 <sup>2</sup> K)	$T_0$ (K)	$R^2$
1.0	0.064 ± 0.030	13.7 ± 1.0	205 ± 4	0.999	0.087 ± 0.013	15.3 ± 0.4	182 ± 1	0.999
0.9	0.063 ± 0.084	13.6 ± 3.0	199 ± 12	0.999	0.047 ± 0.006	13.6 ± 0.3	189 ± 1	0.999
0.8	0.041 ± 0.021	13.4 ± 1.2	198 ± 5	0.999	0.035 ± 0.003	13.2 ± 0.2	188 ± 1	0.999
0.7	0.014 ± 0.002	11.9 ± 2.8	199 ± 1	0.999	0.034 ± 0.004	13.1 ± 0.2	188 ± 1	0.999
0.6	0.012 ± 0.003	11.9 ± 7.0	196 ± 3	0.999	0.023 ± 0.044	12.9 ± 0.4	184 ± 2	0.999
0.5	0.007 ± 0.002	11.0 ± 0.5	195 ± 2	0.999	0.017 ± 0.003	12.3 ± 0.5	184 ± 2	0.999

Supporting Information

## **Ionic Polymer Actuators Using Poly(ionic liquid)s**

Hisashi Kokubo, Ryo Sano, Keita Murai, Shunta Ishii, Masayoshi Watanabe \*

*Department of Chemistry and Biotechnology, Yokohama National University, 79-5 Tokiwadai,  
Hodogaya-ku, Yokohama 240-8501, Japan*

\* Corresponding author

E-mail: mwatanab@ynu.ac.jp

## S1. Experimental details

### S1.1. Instruments

$^1\text{H}$  and  $^{13}\text{C}$  NMR spectra were recorded on a Bruker DRX500 spectrometer using deuterated chloroform ( $\text{CDCl}_3$ ) and deuterated dimethyl sulfoxide ( $\text{DMSO-}d_6$ ) as the solvent. Fourier transform infrared (FT-IR) spectrum was measured on a Nicolet iS50 FT-IR spectrometer by attenuated total reflection (ATR) method.

### S1.2. Materials

Super dehydrated dichloromethane, super dehydrated tetrahydrofuran (THF), super dehydrated *N,N*-dimethylformamide (DMF), and methacryloyl chloride (> 97%) were purchased from Wako Chemical without further purification. 3-Bromo-1-propanol (Sigma-Aldrich), triethylamine (Sigma-Aldrich), lithium bis(trifluoromethanesulfonyl)amide (Morita Chemical Industries), 3-sulfopropyl methacrylate potassium salt (TCI), thionyl chloride (TCI), trifluoromethanesulfonamide (TCI), 1-bromopropane (TCI) were used without further purification. 1-Methylimidazole (TCI) was purified by vacuum distillation prior to use.

### S1.3. Synthesis

#### *S1.3.1 Synthesis of 3-bromopropyl methacrylate*

3-bromo-1-propanol (25.0 g, 169 mmol) was dissolved in dehydrated dichloromethane (40 mL) under an argon atmosphere at 0 °C. A mixture of methacryloyl chloride (16 mL, 169 mmol) and dichloromethane (10 mL) was added into the solution. After stirring for 1 h, triethylamine (23.6 mL,

169 mmol) was added, and the solution was stirred for 24 h at 0 °C. After the filtration of the generated salts, the filtrate was washed water 5 times, and then the solvent was removed by evaporation. A light yellow viscous liquid (25.0 g, 120 mmol, Y = 71%) was obtained after vacuum drying for 12 h at room temperature.  $^1\text{H}$  NMR (500 MHz,  $\text{CDCl}_3$ )  $\delta$ : 6.11 and 5.58 (s, 2H,  $\text{H}_2\text{C}=\text{C}(\text{CH}_3)$ ), 4.29 (t, 2H,  $\text{O}-\text{CH}_2\text{CH}_2\text{CH}_2-\text{Br}$ ), 3.49 (t, 2H,  $\text{O}-\text{CH}_2\text{CH}_2\text{CH}_2-\text{Br}$ ), 2.24 (m, 2H,  $\text{O}-\text{CH}_2\text{CH}_2\text{CH}_2-\text{Br}$ ), 1.95 (s, 3H,  $\text{H}_2\text{C}=\text{C}(\text{CH}_3)$ ).  $^{13}\text{C}$  NMR (125 MHz,  $\text{CDCl}_3$ )  $\delta$ : 167.2 ( $\text{C}=\text{O}$ ), 136.2 ( $\text{CH}_2=\text{C}(\text{CH}_3)$ ), 125.7 ( $\text{CH}_2=\text{C}(\text{CH}_3)$ ), 62.4 ( $\text{O}-\text{CH}_2\text{CH}_2\text{CH}_2-\text{Br}$ ), 31.8 ( $\text{O}-\text{CH}_2\text{CH}_2\text{CH}_2-\text{Br}$ ), 29.4 ( $\text{O}-\text{CH}_2\text{CH}_2\text{CH}_2-\text{Br}$ ), 18.3 ( $\text{CH}_2=\text{C}(\text{CH}_3)$ ).

### 51.3.2. Synthesis of $[\text{C}_3\text{mim-MA}]\text{Br}$

7.7 mL of 1-methylimidazole (96.6 mmol) was dropped into 20.0 g of 3-bromopropyl methacrylate (96.6 mmol) in a three-necked round-bottom flask under argon atmosphere at 0 °C, and the reaction solution was stirred for 12 h at 0 °C and then stirred for 12 h at room temperature. The obtained powder was washed with diethyl ether. After vacuum drying for 24 h at room temperature, white powder was obtained (21.0 g, 72.6 mmol, Y = 75%).  $^1\text{H}$  NMR (500 MHz,  $\text{CDCl}_3$ )  $\delta$ : 10.36 (s, 1H,  $\text{N}-\text{CH}=\text{N}$ ), 7.63 and 7.60 (s, 2H,  $\text{N}-\text{CH}=\text{CH}-\text{N}$ ), 6.10 and 5.61 (s, 2H,  $\text{H}_2\text{C}=\text{C}(\text{CH}_3)$ ), 4.53 (t, 2H,  $\text{O}-\text{CH}_2\text{CH}_2\text{CH}_2-\text{N}$ ), 4.26 (t, 2H,  $\text{O}-\text{CH}_2\text{CH}_2\text{CH}_2-\text{N}$ ), 4.12 (s, 3H,  $\text{N}-\text{CH}_3$ ), 2.41 (m, 2H,  $\text{O}-\text{CH}_2\text{CH}_2\text{CH}_2-\text{N}$ ), 1.93 (s, 3H,  $\text{H}_2\text{C}=\text{C}(\text{CH}_3)$ ).  $^{13}\text{C}$  NMR (125 MHz,  $\text{CDCl}_3$ )  $\delta$ : 167.2 ( $\text{C}=\text{O}$ ), 137.7 and 135.8 ( $\text{CH}_2=\text{C}(\text{CH}_3)$  and  $\text{N}-\text{CH}=\text{N}$ ), 126.4 ( $\text{CH}_2=\text{C}(\text{CH}_3)$ ), 123.6 and 122.6 ( $\text{N}-\text{CH}=\text{CH}-\text{N}$ ), 61.0 ( $\text{O}-\text{CH}_2\text{CH}_2\text{CH}_2-\text{N}$ ), 47.3 ( $\text{O}-\text{CH}_2\text{CH}_2\text{CH}_2-\text{N}$ ), 36.9 ( $\text{N}-\text{CH}_3$ ), 29.7 ( $\text{O}-\text{CH}_2\text{CH}_2\text{CH}_2-\text{N}$ ), 18.3

(CH<sub>2</sub>=C(CH<sub>3</sub>)).

### S1.3.3. Synthesis of [C<sub>3</sub>mim-MA][TFSA]

50 mL of an aqueous solution of [C<sub>3</sub>mim-MA]Br (20.0 g, 69.1 mmol) was dropped into 50 mL of an aqueous solution of Li[TFSA] (28.4 g, 98.8 mmol) at room temperature and the solution was stirred for 12 h. The phase separated layer was dissolved in dichloromethane, and washed with water several times until the water phase did not become cloudy by the addition of a silver nitrate aqueous solution. After evaporation of the dichloromethane, vacuum drying was conducted for 12 h at room temperature to afford [C<sub>3</sub>mim-MA][TFSA] as a colorless oily liquid (21.2g, 43 mmol, Y = 52%). <sup>1</sup>H NMR (500 MHz, CDCl<sub>3</sub>) δ: 8.76 (s, 1H, N-CH-N), 7.39 and 7.32 (s, 2H, N-CH=CH-N), 6.08 and 5.61 (s, 2H, H<sub>2</sub>C=C(CH<sub>3</sub>)), 4.30 (t, 2H, O-CH<sub>2</sub>CH<sub>2</sub>CH<sub>2</sub>-N), 4.21 (t, 2H, O-CH<sub>2</sub>CH<sub>2</sub>CH<sub>2</sub>-N), 3.93 (s, 3H, N-CH<sub>3</sub>), 2.28 (m, 2H, O-CH<sub>2</sub>CH<sub>2</sub>CH<sub>2</sub>-N), 1.92 (s, 3H, H<sub>2</sub>C=C(CH<sub>3</sub>)). <sup>13</sup>C NMR (125 MHz, CDCl<sub>3</sub>) δ: 167.2 (COO), 136.4 and 135.7 (CH<sub>2</sub>=C(CH<sub>3</sub>) and N-CH-N), 126.3 (CH<sub>2</sub>=C(CH<sub>3</sub>)), 123.8 and 122.6 (N-CH=CH-N), 121.5 and 118.5 and 116.0 (CF<sub>3</sub>), 60.7 (O-CH<sub>2</sub>CH<sub>2</sub>CH<sub>2</sub>-N), 47.3 (O-CH<sub>2</sub>CH<sub>2</sub>CH<sub>2</sub>-N), 36.4 (N-CH<sub>3</sub>), 29.3 (O-CH<sub>2</sub>CH<sub>2</sub>CH<sub>2</sub>-N), 18.1 (CH<sub>2</sub>=C(CH<sub>3</sub>)).

### S1.3.4. Synthesis of 3-(chlorosulfonyl)propyl methacrylate

Thionyl chloride (40.5 mL, 547 mmol) was dropped into a suspension mixture of 3-sulfopropyl methacrylate potassium salt (25.0 g, 99.5 mmol), dehydrated THF (60 mL), and dehydrated DMF (2.56 mL) (as a reaction catalyst) spending 1 h under argon atmosphere at 0 °C. After stirring for 12

h at 0 °C, the reaction mixture was poured into a large amount of water (ca. 400 mL) to remove the unreacted thionyl chloride and generated potassium chloride. The phase separated layer was dissolved in dichloromethane and washed with water 5 times. After drying with magnesium sulfate, the dichloromethane was removed by evaporation and dried under vacuum at room temperature to afford 3-(chlorosulfonyl)propyl methacrylate (20.5 g, 90.4 mmol, Y = 91%) as a light yellow liquid. <sup>1</sup>H NMR (500 MHz, CDCl<sub>3</sub>) δ: 6.13 and 5.63 (s, 2H, H<sub>2</sub>C=C(CH<sub>3</sub>)), 4.34 (m, 2H, O-CH<sub>2</sub>CH<sub>2</sub>CH<sub>2</sub>-S), 3.79 (m, 2H, O-CH<sub>2</sub>CH<sub>2</sub>CH<sub>2</sub>-S), 2.45 (m, 2H, O-CH<sub>2</sub>CH<sub>2</sub>CH<sub>2</sub>-S), 1.96 (s, 3H, H<sub>2</sub>C=C(CH<sub>3</sub>)). <sup>13</sup>C NMR (125 MHz, CDCl<sub>3</sub>) δ: 166.9 (COO), 135.7 (CH<sub>2</sub>=C(CH<sub>3</sub>)), 126.4 (CH<sub>2</sub>=C(CH<sub>3</sub>)), 62.3 (O-CH<sub>2</sub>CH<sub>2</sub>CH<sub>2</sub>-S), 61.3 (O-CH<sub>2</sub>CH<sub>2</sub>CH<sub>2</sub>-S), 24.2 (O-CH<sub>2</sub>CH<sub>2</sub>CH<sub>2</sub>-S), 18.2 (CH<sub>2</sub>=C(CH<sub>3</sub>)).

#### SI.3.5. Synthesis of [N<sub>0222</sub>][TFSA-MA]

Triethylamine (27.1 mL, 194 mmol) was added in 50 mL of a dehydrated THF solution of trifluoromethanesulfonyl amide (13.1 g, 88.2 mmol) under argon atmosphere at 0 °C. Dehydrated THF (10 mL) solution of 3-(chlorosulfonyl)propyl methacrylate (20.0 g, 88.2 mmol) kept at 0 °C was dropped into the reaction solution spending 1 h, and the mixture was stirred for 2h at 0 °C. The generated triethylammonium chloride was removed by filtration. After evaporation of THF from the filtrate, the remaining solid was dissolved in dichloromethane. The solution was washed with water of 0 °C 3 times, and drying was conducted with magnesium sulfate. After removal of dichloromethane, vacuum drying was carried out for 4 h at room temperature to give [N<sub>0222</sub>][TFSA-MA] as a yellow liquid (16.7 g, 37.9 mmol, Y = 43%). <sup>1</sup>H NMR (500 MHz,

DMSO-*d*<sub>6</sub>)  $\delta$ : 8.82 (br, 1H, H-N), 6.04 and 5.68 (s, 2H, H<sub>2</sub>C=C(CH<sub>3</sub>)), 4.18 (m, 2H, O-CH<sub>2</sub>CH<sub>2</sub>CH<sub>2</sub>-S), 3.10 (m, 6H, N-CH<sub>2</sub>CH<sub>3</sub>), 3.06 (t, 2H, O-CH<sub>2</sub>CH<sub>2</sub>CH<sub>2</sub>-S), 2.02 (m, 2H, O-CH<sub>2</sub>CH<sub>2</sub>CH<sub>2</sub>-S), 1.88 (s, 3H, H<sub>2</sub>C=C(CH<sub>3</sub>)), 1.18 (t, 9H, N-CH<sub>2</sub>CH<sub>3</sub>). <sup>13</sup>C NMR (125 MHz, DMSO-*d*<sub>6</sub>)  $\delta$ : 166.4 (COO), 135.8 (CH<sub>2</sub>=C(CH<sub>3</sub>)), 125.7 (CH<sub>2</sub>=C(CH<sub>3</sub>)), 121.4 and 118.8 and 116.2 (CF<sub>3</sub>), 62.7 (O-CH<sub>2</sub>CH<sub>2</sub>CH<sub>2</sub>-S), 51.2 (O-CH<sub>2</sub>CH<sub>2</sub>CH<sub>2</sub>-S), 45.8 (N-CH<sub>2</sub>CH<sub>3</sub>), 23.5 (O-CH<sub>2</sub>CH<sub>2</sub>CH<sub>2</sub>-S), 17.9 (CH<sub>2</sub>=C(CH<sub>3</sub>)), 8.7 (N-CH<sub>2</sub>CH<sub>3</sub>).

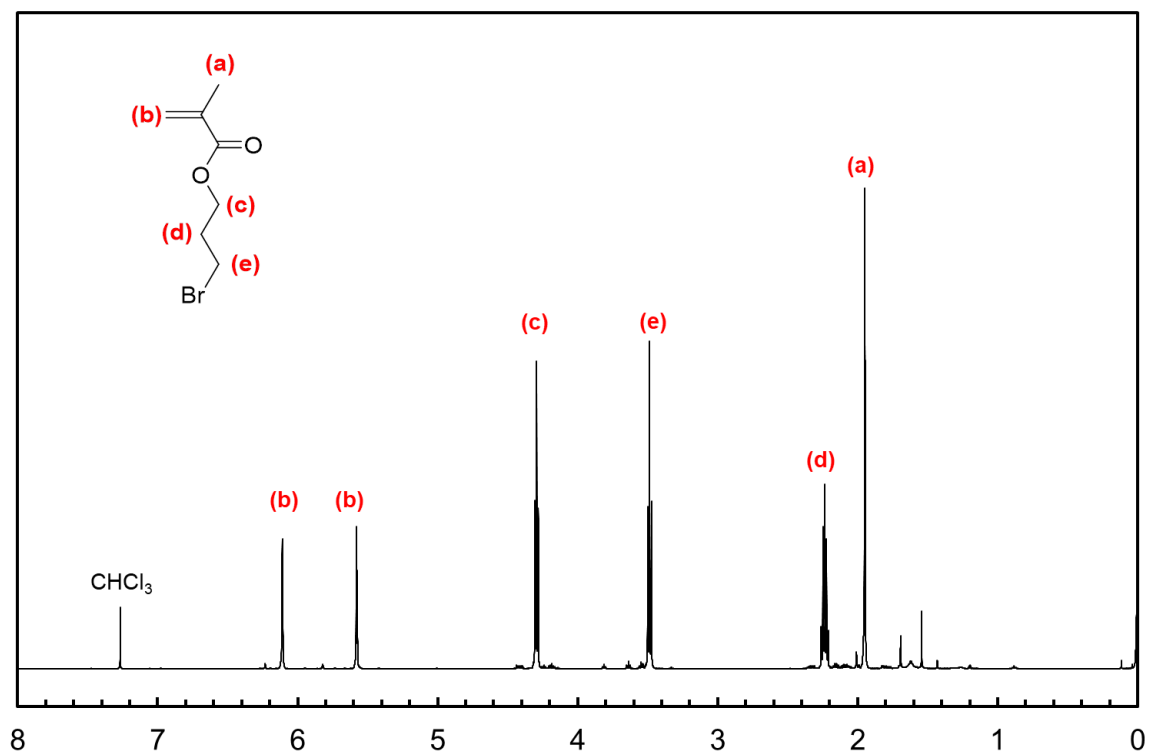


**Fig. S1**  $^1\text{H}$  NMR spectrum of 3-bromopropyl methacrylate in  $\text{CDCl}_3$ .

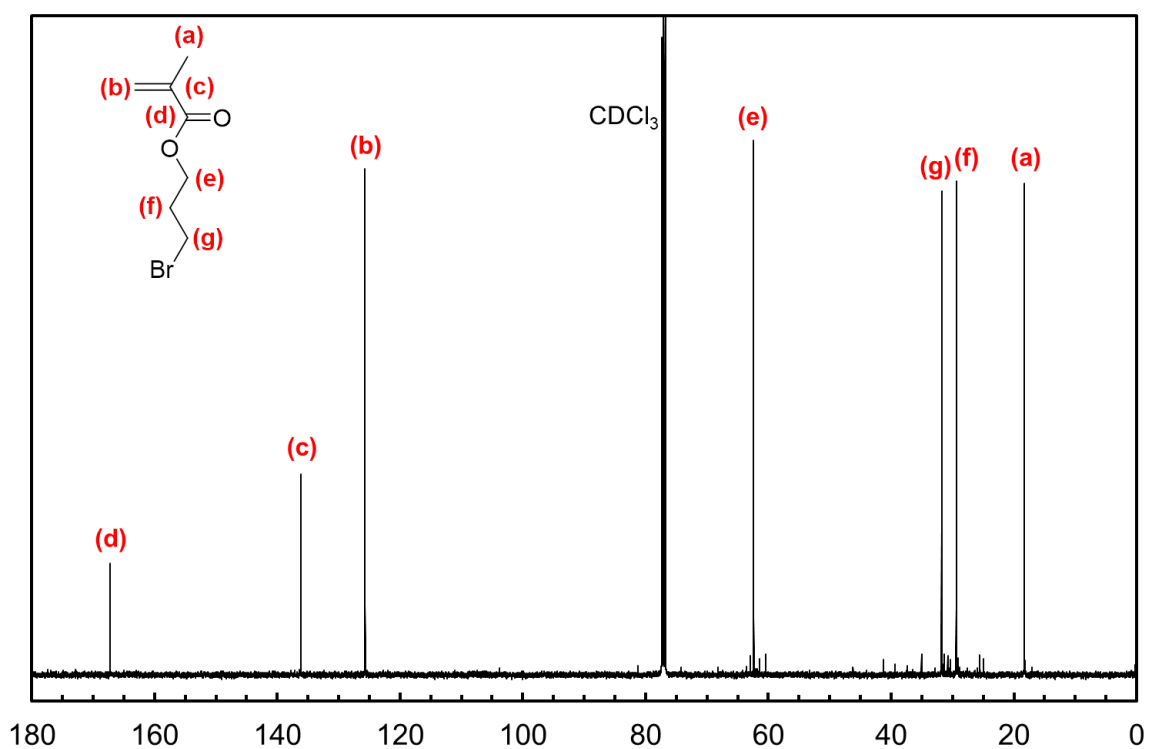


**Fig. S2**  $^{13}\text{C}$  NMR spectrum of 3-bromopropyl methacrylate in  $\text{CDCl}_3$ .

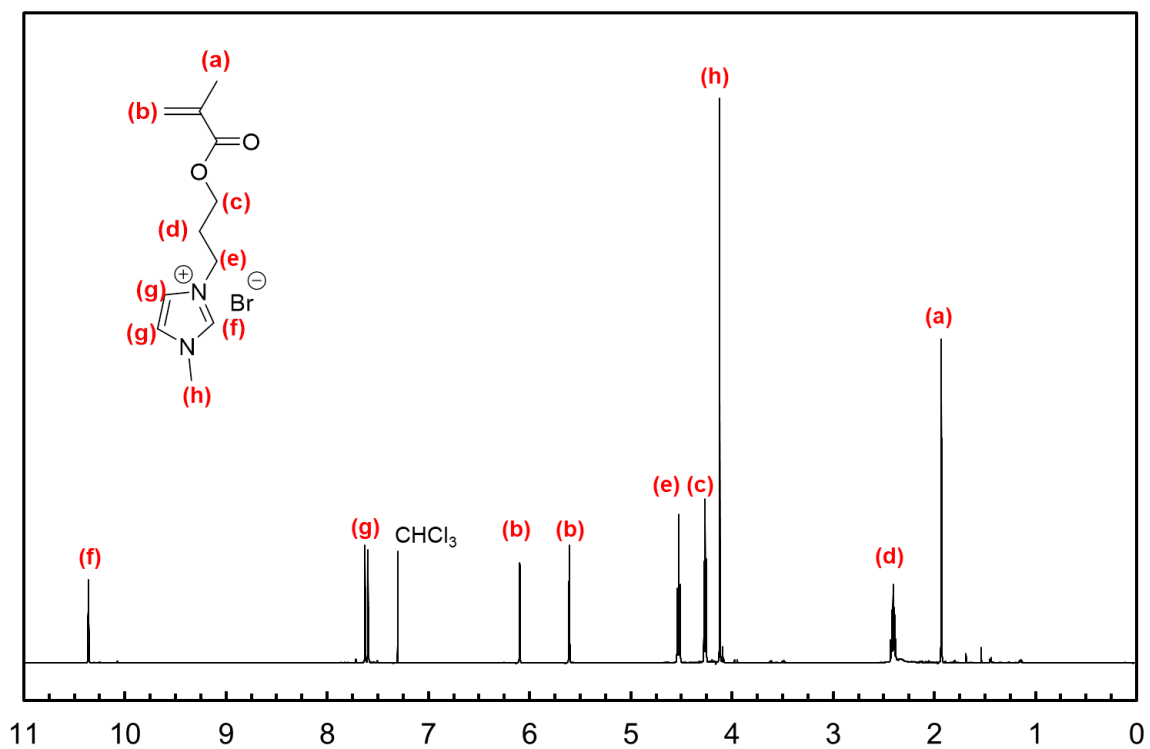


Fig. S3  $^1\text{H}$  NMR spectrum of  $[\text{C}_3\text{mim-MA}]\text{Br}$  in  $\text{CDCl}_3$ .

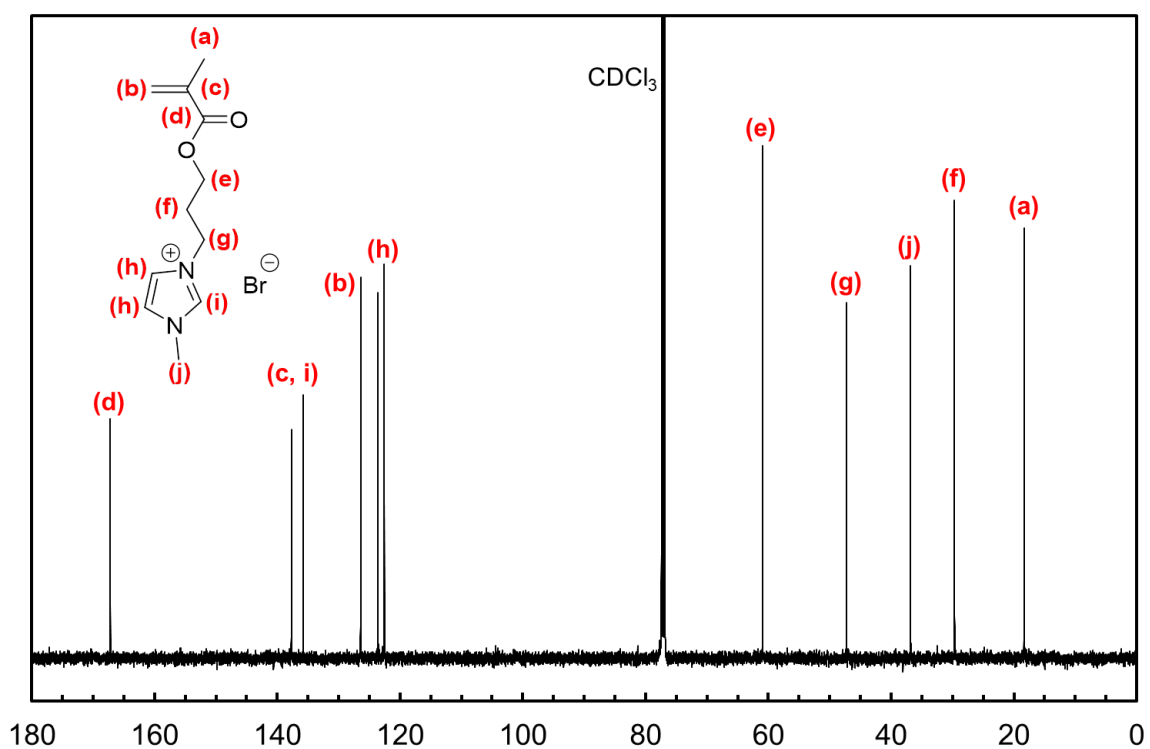


Fig. S4  $^{13}\text{C}$  NMR spectrum of  $[\text{C}_3\text{mim-MA}]\text{Br}$  in  $\text{CDCl}_3$ .

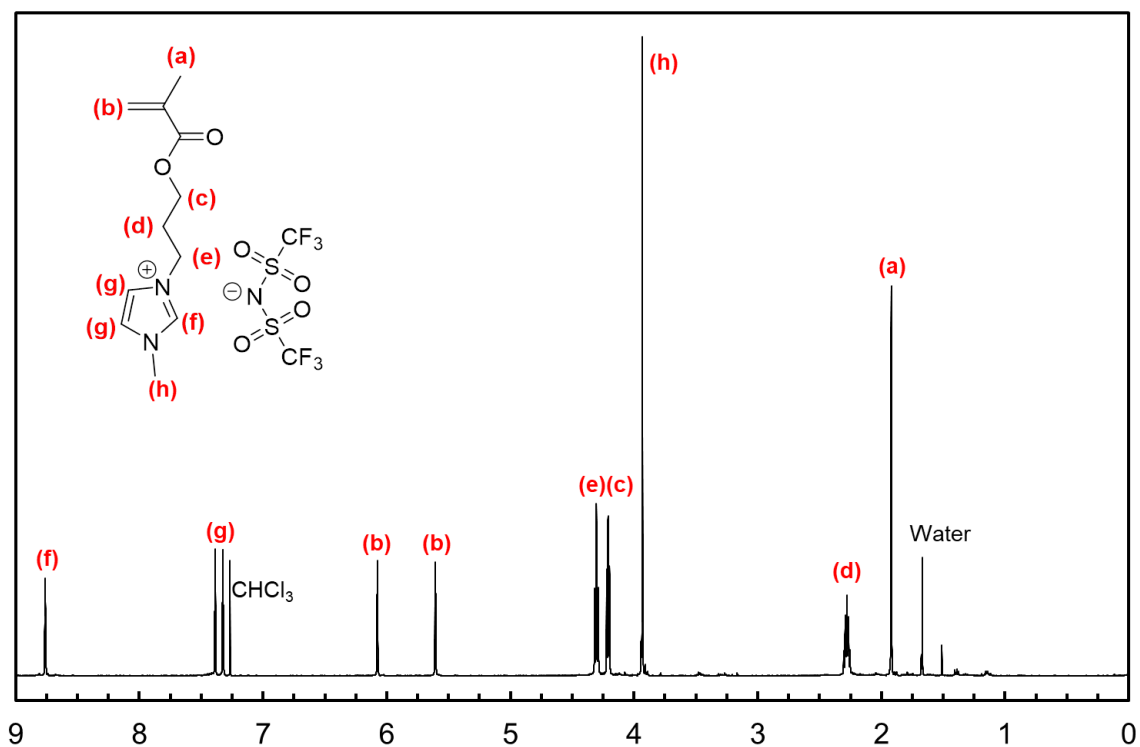


Fig. S5  $^1\text{H}$  NMR spectrum of  $[\text{C}_3\text{mim-MA}][\text{TfSA}]$  in  $\text{CDCl}_3$ .

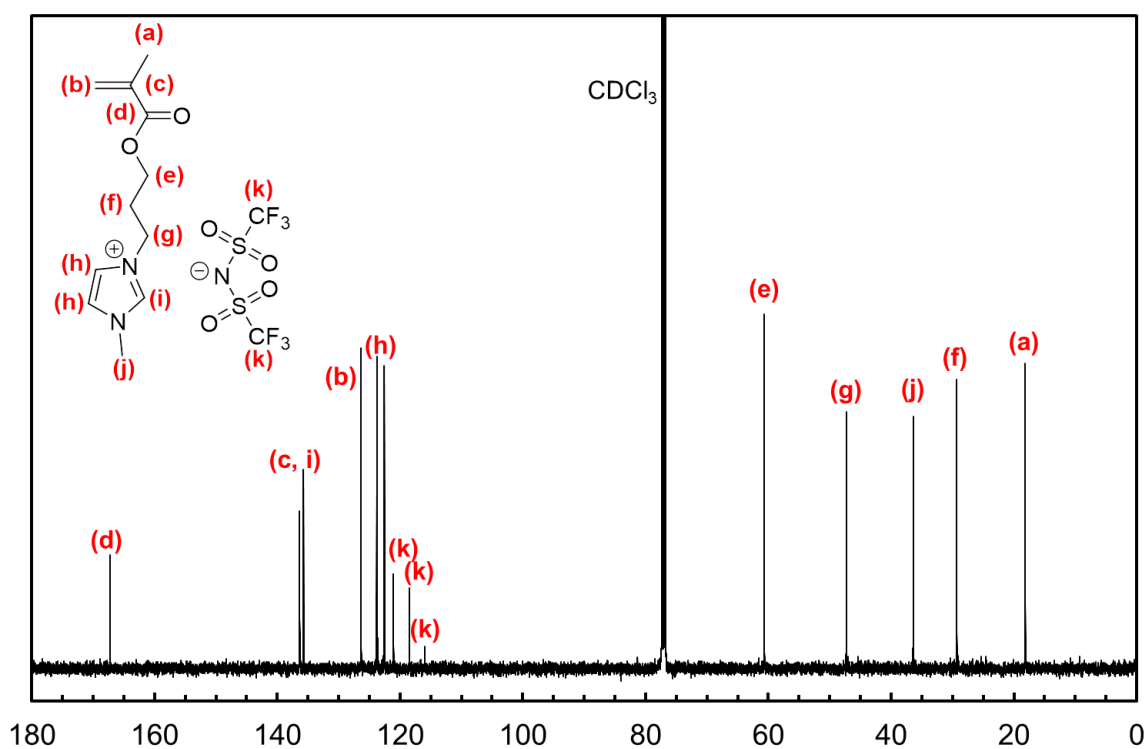
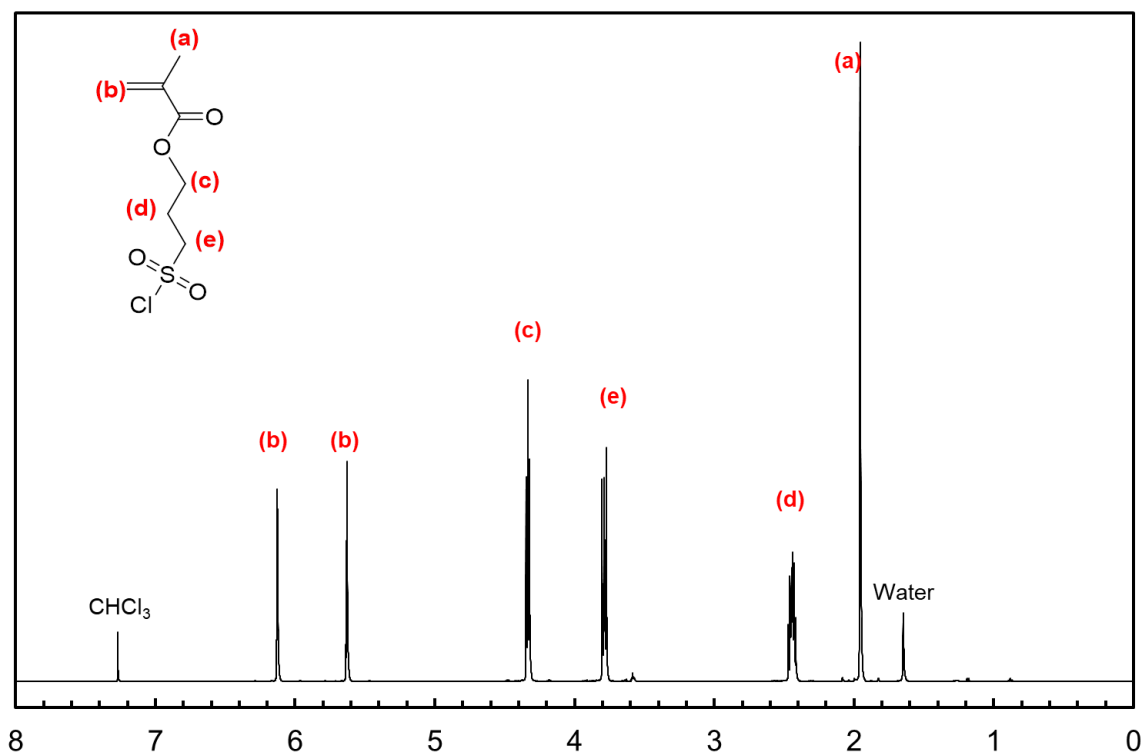
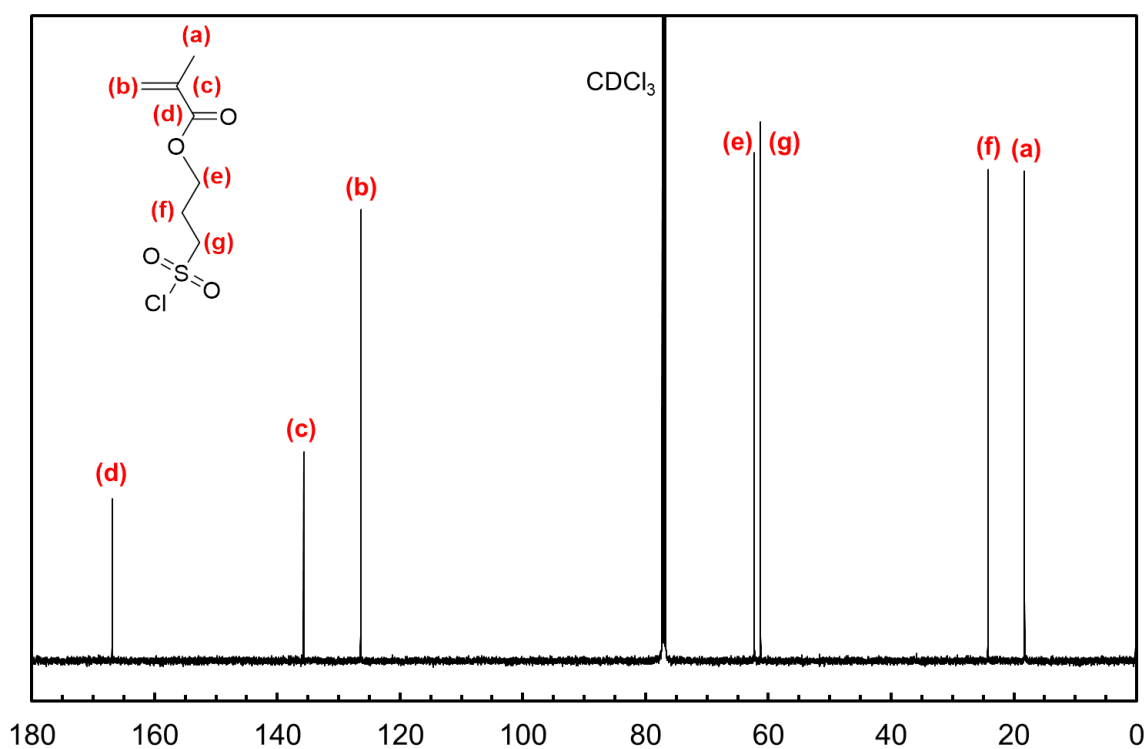


Fig. S6  $^{13}\text{C}$  NMR spectrum of  $[\text{C}_3\text{mim-MA}][\text{TfSA}]$  in  $\text{CDCl}_3$ .



**Fig. S7** <sup>1</sup>H NMR spectrum of 3-(chlorosulfonyl)propyl methacrylate in CDCl<sub>3</sub>.



**Fig. S8** <sup>13</sup>C NMR spectrum of 3-(chlorosulfonyl)propyl methacrylate in CDCl<sub>3</sub>.

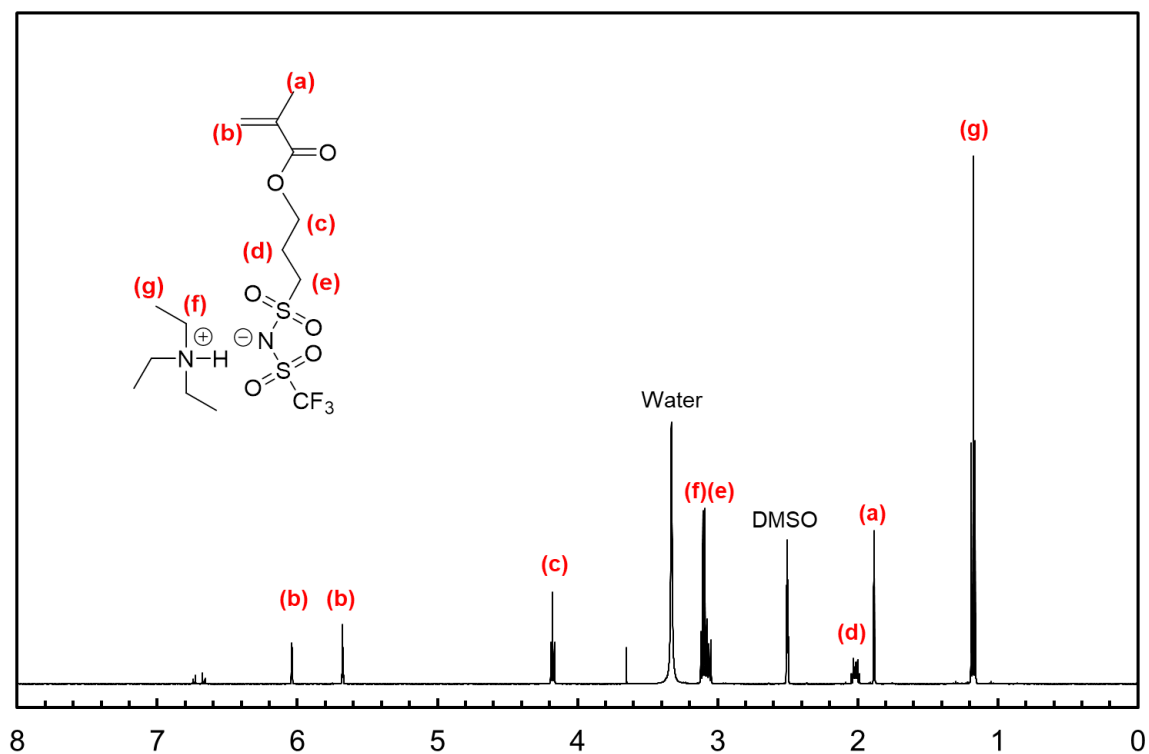


**Fig. S9**  $^1\text{H}$  NMR spectrum of  $[\text{N}_{0222}][\text{TFSA-MA}]$  in  $\text{DMSO-}d_6$ .

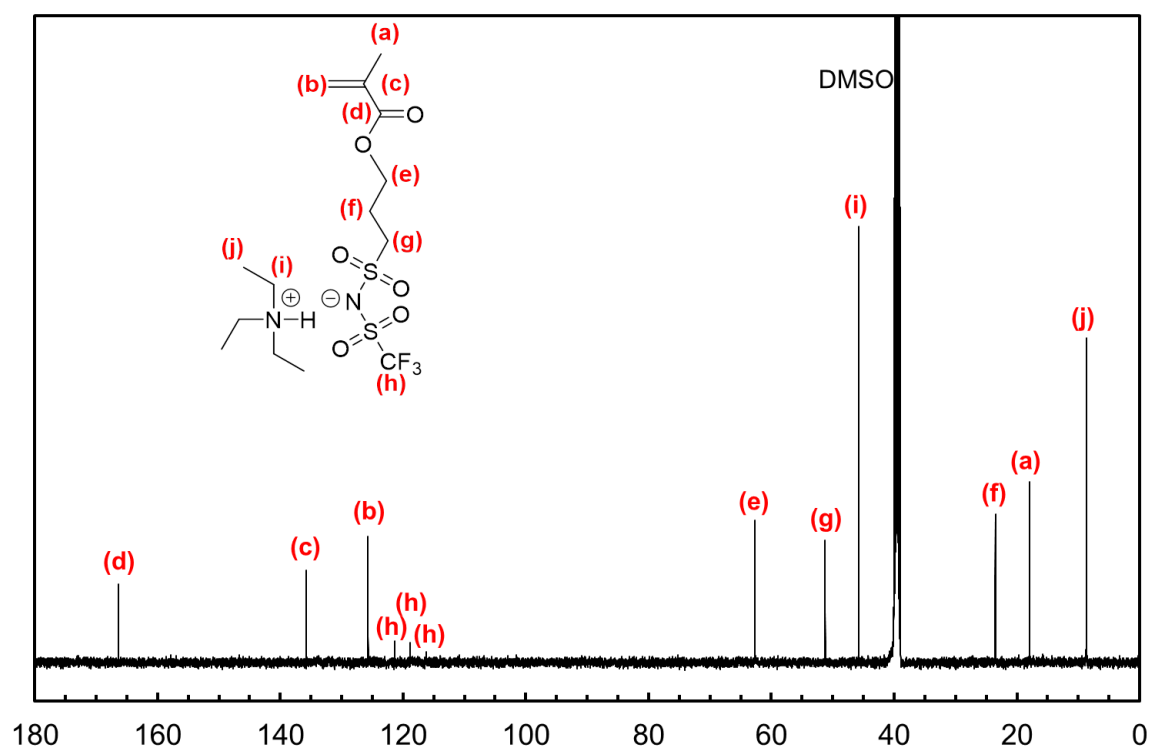


**Fig. S10**  $^{13}\text{C}$  NMR spectrum of  $[\text{N}_{0222}][\text{TFSA-MA}]$  in  $\text{DMSO-}d_6$ .

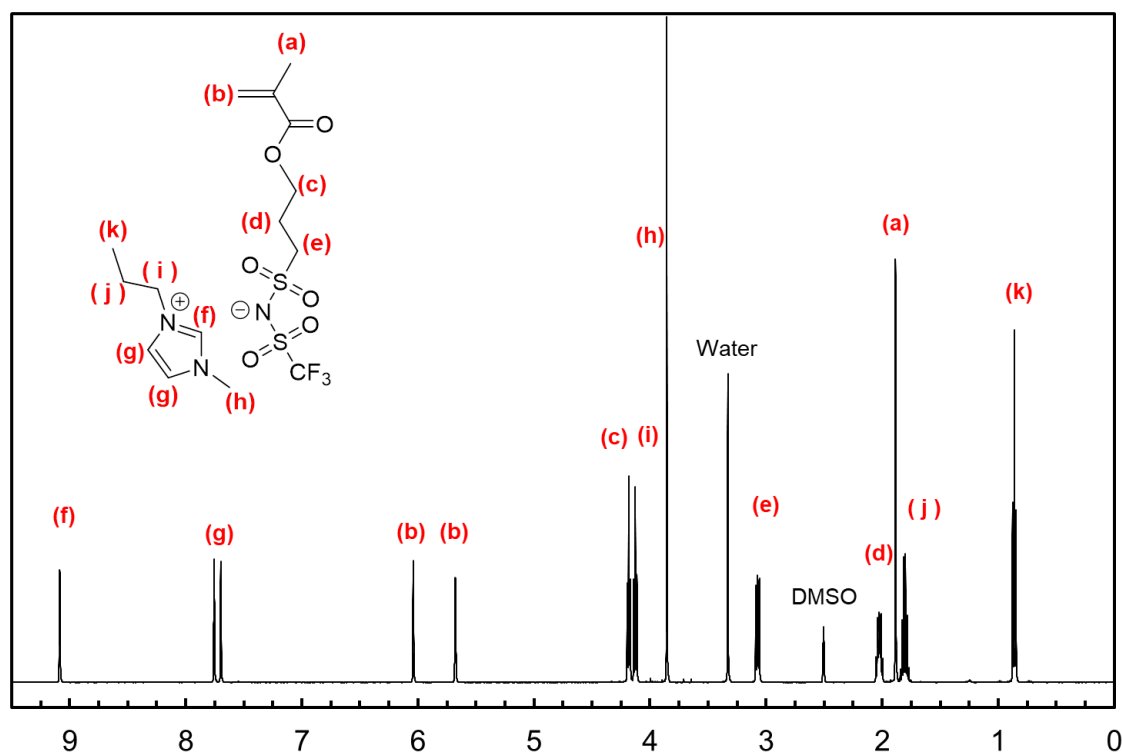


Fig. S11  $^1\text{H}$  NMR spectrum of  $[\text{C}_3\text{mim}][\text{TFSA-MA}]$  in  $\text{DMSO-}d_6$ .

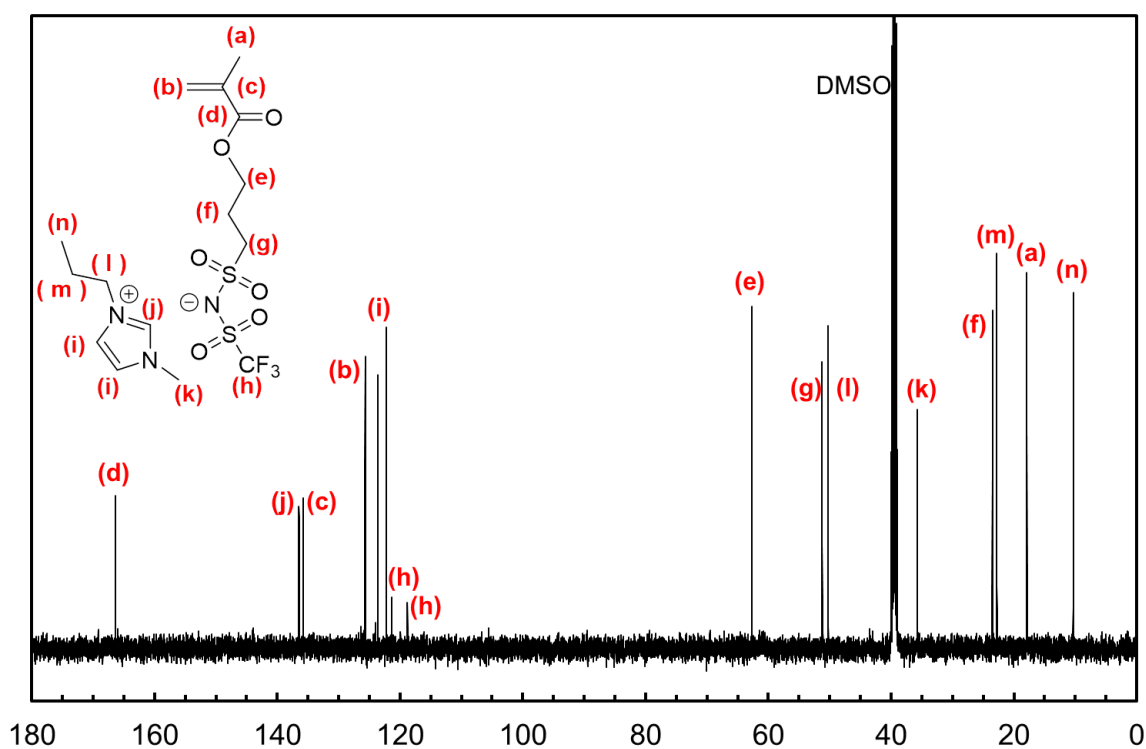
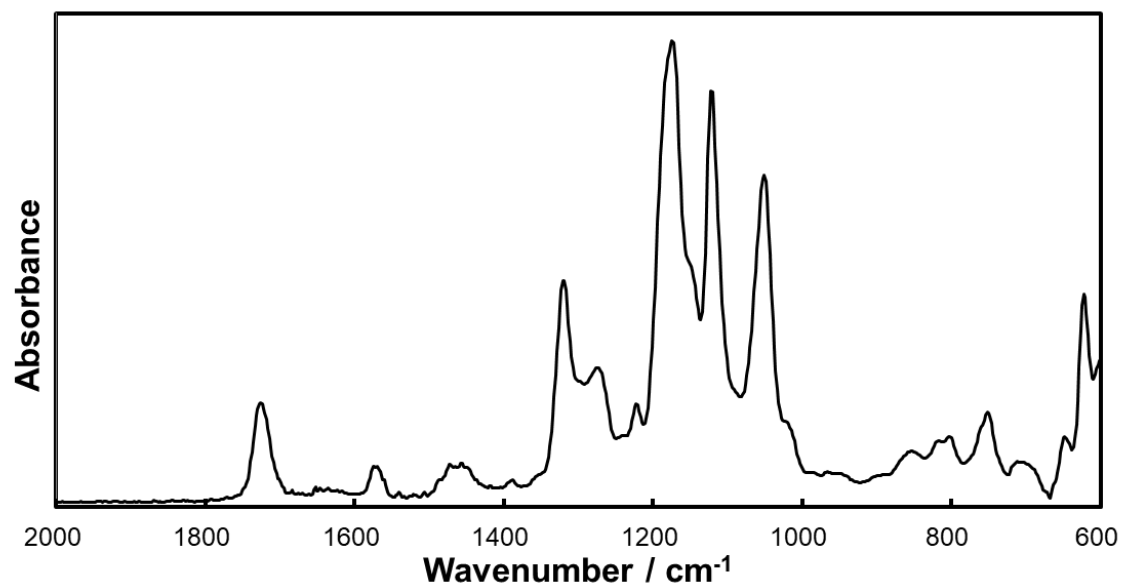
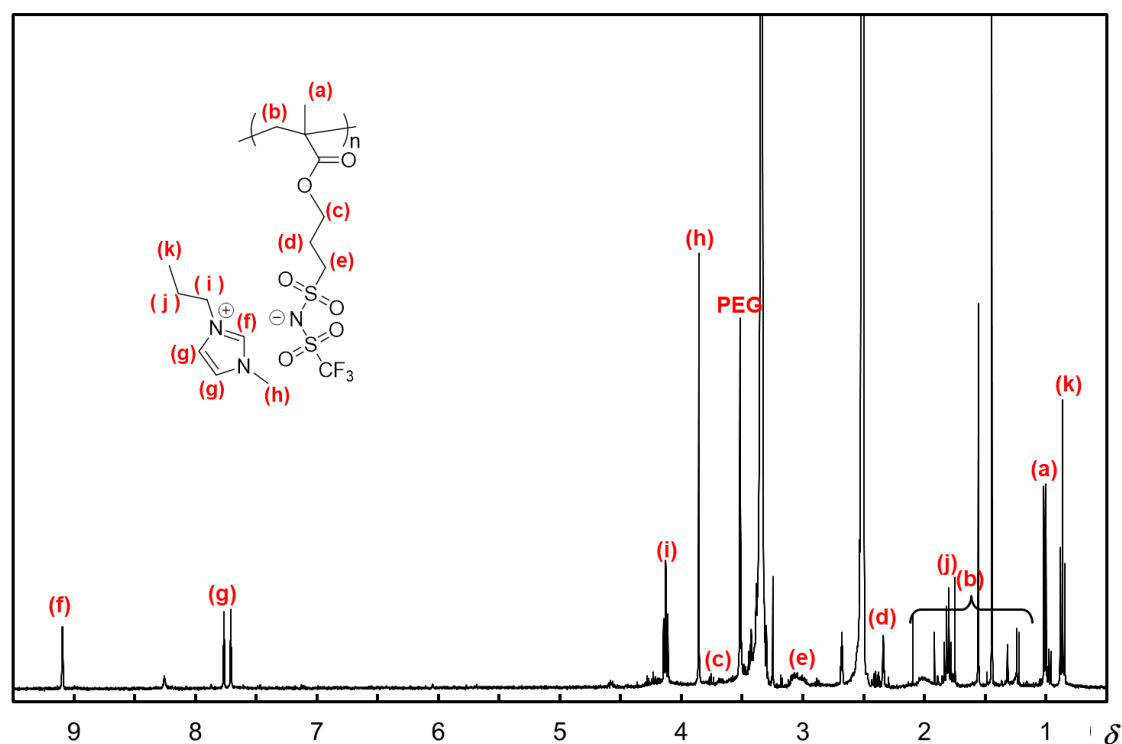


Fig. S12  $^{13}\text{C}$  NMR spectrum of  $[\text{C}_3\text{mim}][\text{TFSA-MA}]$  in  $\text{DMSO-}d_6$ .



**Fig. S13** FT-IR spectrum of polyanion network with  $x$  value of 0.9.



**Fig. S14**  $^1\text{H}$  NMR spectrum of a  $\text{DMSO-}d_6$  solution of polyanion network extract. The  $x$  value of the polymer network is 0.9. The measured solution was prepared by soaking of polyanion network (ca. 50 mg) in  $\text{DMSO-}d_6$  (2 mL) for 12 h with gentle shaking.

**Table S1** Feed compositions of the reagents for preparation of polycation

$x^a$	[C <sub>3</sub> mim-MA][TFSA] / g (mmol)	PEGMEM / $\mu$ L (mmol)	AIBN / mg ( $\mu$ mol)	EGDMA / $\mu$ L ( $\mu$ mol)
1.0	2.00 (4.09)	0 (0.00)	13.4 (81.7)	15.4 (81.6)
0.9	1.80 (3.68)	185 (0.40)	13.4 (81.7)	15.4 (81.6)
0.8	1.60 (3.27)	370 (0.80)	13.4 (81.7)	15.4 (81.6)
0.7	1.40 (2.86)	556 (1.20)	13.3 (81.2)	15.3 (81.0)
0.6	1.20 (2.45)	740 (1.60)	13.3 (81.2)	15.3 (81.0)
0.5	1.00 (2.04)	926 (2.00)	13.3 (81.2)	15.3 (81.0)

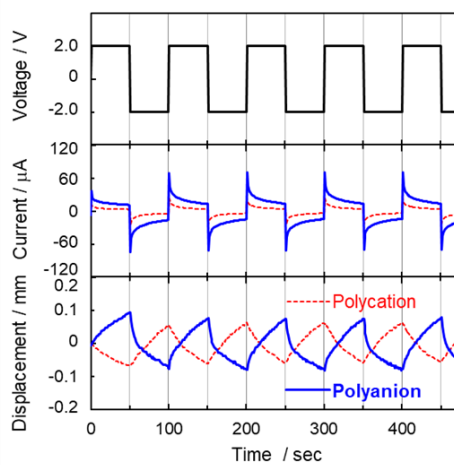
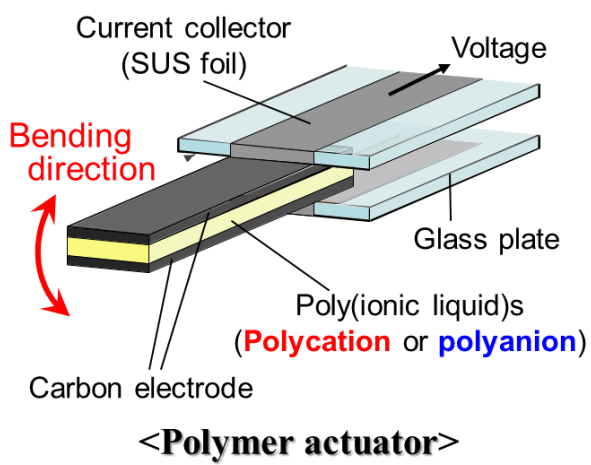
a) Weight ratio of [C<sub>3</sub>mim-MA][TFSA] to all monomers except for crosslinker.

**Table S2** Feed compositions of the reagents for preparation of polyanion

$x^a$	[C <sub>3</sub> mim][TFSA-MA] / mg ( $\mu$ mol)	PEGMEM / $\mu$ L ( $\mu$ mol)	AIBN / mg ( $\mu$ mol)	EGDMA / $\mu$ L ( $\mu$ mol)
1.0	2.00 (4.32)	0 (0.00)	14.1 (86.3)	16.2 (86.2)
0.9	1.80 (3.88)	185 (0.40)	14.1 (85.7)	16.1 (85.6)
0.8	1.60 (3.45)	370 (0.80)	14.0 (85.1)	16.0 (85.0)
0.7	1.40 (3.02)	556 (1.20)	13.9 (84.4)	15.9 (84.4)
0.6	1.20 (2.59)	740 (1.60)	13.8 (83.8)	15.8 (83.8)
0.5	1.00 (2.16)	926 (2.00)	13.7 (83.2)	15.7 (83.2)

a) Weight ratio of [C<sub>3</sub>mim][TFSA-MA] to all monomers except for crosslinker.

## Graphical Abstract



**Highlights**

- Poly(ionic liquid) (polyIL) networks were prepared via free radical polymerization.
- The polyILs have either imidazolium or  $-\text{[SO}_2\text{NSO}_2\text{CF}_3\text{]}^-$  structure in their side chains as the fixed charge.
- Ionic polymer actuators with the polyIL network electrolyte layer showed a characteristic performance depending on the fixed charge on the network.